Survey of calculations on the Haddam Neck (Connecticut Yankee) power plant as a test of the Risø Reactor Physics code system

Neltrup, H.; Suhr, P.B.

Publication date:
1973

Document Version
Publisher's PDF, also known as Version of record

Risø Report No. 298

Risø Report No. 298

Danish Atomic Energy Commission

Research Establishment Risø

Survey of Calculations on the Haddam Neck (Connecticut Yankee) Power Plant as a Test of the Risø Reactor Physics Code System

by H. Neltrup and Per B. Suhr

August 1973

Sales distributors: Jul. Gjellerup, 87, Sølvgade, DK-1307 Copenhagen K, Denmark

Available on exchange from: Library, Danish Atomic Energy Commission, Risø, DK-4000 Roskilde, Denmark

August 1973 Risø Report No. 298

Survey of Calculations on the Haddam Neck (Connecticut Yankee) Power Plant as a Test of the Risø Reactor Physics Code System

by

H. Neltrup and Per B. Suhr

Danish Atomic Energy Commission
Research Establishment Risø
Reactor Physics Department

UDC 621.039.51 : 621.039.44 : 681.3.06

Abstract

A summary is presented of the stationary and quasistationary calculations carried out on the first core loading of the CONNECTICUT YANKEE ATOMIC POWER CO HADDAM NECK POWER PLANT as a test of the Reactor Physics Department computer code system.

The calculations described include calculations of criticality, reactivity coefficients, poison coefficients, differential and integral values of the control rod system, and power distributions during burn-up.

INIS Descriptors

BURNUP
COMPUTER CALCULATIONS
CONNECTICUT YANKEE REACTOR
CONTROL ROD WORTHS
CROSS SECTIONS
DANCOFF CORRECTION
FLUX SYNTHESIS
FUEL ELEMENTS
GROUP CONSTANTS
MULTIGROUP THEORY
NEUTRON DIFFUSION EQUATION
REACTIVITY COEFFICIENTS
THREE-DIMENSIONAL CALCULATIONS
TWO-DIMENSIONAL CALCULATIONS

ISBN 87 550 0228 5

CONTENTS

Page

1. INTRODUCTION

The present report describes some of the stationary and quasistationary calculations carried out on the CONNECTICUT YANKEE ATOMIC POWER CO HADDAM NECK POWER PLANT, a Westinghouse pressurized-water reactor with a thermal power level of 1825 MW_{th} (600 MW gross electrical).

The purpose of the project was to verify parts of the Risø reactor physics computer code system, not only with regard to calculations of core performance, but also to obtaining experience with the system used on calculations with safety aspects as reactivity coefficients, differential and integral values of different groups of control rods, and boron worth.

The Westinghouse Connecticut Yankee was chosen as a literature study had shown this reactor suitable because of the accessibility of information on geometrical data, composition, measurements, and calculation results[1-6].

The Risø code system in its present version has previously been tested against calculations on the DRESDEN boiling-water reactor[7-8].

2. THE RISØ REACTOR PHYSICS COMPUTING PROGRAM SYSTEM

The codes described below are coded for the Risø Burroughs Computer B 6700.

Fig. 2.a shows those parts of the Risø reactor physics code complex which are of interest for the calculations described in this report. In the following a short description of the modules shown in the figure is given. A more detailed description and verification of the code complex are given in refs. 7-11.

2.1. The Data Libraries

Two main sources with detailed cross sections are used: the UKNDL 1968 nuclear data library[12-13] and the RESAB[14] resonance parameter library for resonance nuclides in fuel, control absorbers, burnable poisons and important fission products.

The first processing step is performed by the program SIGMA[15] built over the same pattern as the UK program GALAXY. As this step is very time-consuming, it was found necessary to establish a library, the SIGMA MASTER TAPE[16], containing fine group cross sections produced by SIGMA. At present it contains fine group cross sections for 126 isotopes including 78 fission products.

2.2. Self-shielded Cross Sections

Parallel processing of self-shielded, temperature dependent group cross sections is performed by the RESAB program system, either by semianalytical methods e.g. when calculating statistical region and p-wave contributions, or by numerical methods similar to those used in the UK program SDR[17] involving multiregion collision probability methods in several thousand energy groups. In the important resolved region this method effectively copes with the spatial effects and also with the overlap of several resonance nuclides.

In many cases, however, sufficient accuracy can be obtained by means of a suitable equivalence principle combined with interpolation in tabulated group resonance integrals precalculated by RESAB. Interpolation parameters are temperature and excess scattering.

Resonance overlap corresponding to a suitable standard concentration of the three nuclides ^{235}U, ^{238}U, and ^{239}Pu has been incorporated in the tables. Simple concentration dependent overlap corrections[18] are made on the interpolated value. This procedure has been included in the subroutine RESOREX[19].

2.3. The Group Structure

It is important in the fine group set produced by the first processing step to have a sufficiently fine structure so as to make the group cross sections insensitive to variations of the spectrum since only its coarser features are known at this stage.

In the resonance region, however, improved accuracy and reduced number of groups may be obtained as reported in ref. 18 by choosing broader groups in which the dominant resonances are either situated in the centre of or evenly spaced in the lethargy interval of the corresponding group.

On the basis of these considerations a 76-group system was set up. The structure of the 35 thermal groups was taken over directly from the LASER code[9]. The main feature of this well-known group set is the clustering of narrow groups around the 0.3 eV ^{239}Pu and the 1 eV ^{240}Pu resonances.

2.4. Condensation of Cross Sections

The program complex CRS[11] uses fine group cross sections from the master tape and RESAB or RESOREX and supplements with thermal scattering matrices from the subroutine NELKIN SCM. CRS calculates the fine group spectrum either in a specified homogeneous medium or in the subroutine GP by use of multiregion collision probability methods in a specified cylinder or slab cell.

The GP routine may also be used as an independent program and is used as such in connection with control rod calculations (see fig. 2.a).

The fine group spectrum is used to condense cross sections in energy and space to a prescribed group structure.

For use in the box program CDB, the 76 groups are condensed to 10 or 5 groups respectively for the pin cell collision probability routine and the diffusion theory overall box calculation.

2.5. Fuel Box Calculations

The fuel box code CDB[9] may handle fuel pins of different radii and compositions, non-burnable regions, e.g. water gaps, control rods of circular or rectangular shape, and burnable poisons. The program combines the unit cell flux distribution and burn-up calculations (collision probability calculations) and a two-dimensional diffusion theory flux solution for the fuel element (and its surrounding water gaps), yielding power distributions, isotopic concentrations, box average cross sections, etc. as functions of the burn-up.

The collision probability calculations are carried out in regions specified as pin cells and characterized by a number of concentric subregions provided with multigroup cross sections, in most cases 10-group cross sections.

The reflection of neutrons on the surface of the pin cells is adjusted by an iterative process to match the in- or out-leakage through the surface as determined by the overall (box) flux.

From the cell fluxes calculated in this way homogenized and condensed few-group - in most cases 5-group - cross sections are calculated for use in the overall diffusion theory box calculations.

Other regions such as control rods, water gaps, holes, and shrouds or a combination of these are specified as homogeneous regions and are provided directly with few (5)-group cross sections for diffusion theory calculations.

When by iteration between pin cell and box overall calculations a sufficient degree of convergence has been obtained, homogenization and further condensation based on the box-overall calculation is carried out to derive

effective few-group - in most cases 2-group - cross sections for the entire box.

Burn-up calculations may be performed on the 10-group level in all fuel bearing pin cells and detailed information on isotope compositions as well as homogenized few-group cross sections for the entire box may be printed out and punched on cards at every burn-up step.

2.6. Overall Calculations

The program DIFF 2D solves the diffusion theory equation in (x, y) or (r, z) geometry by difference methods. The DBU program[9] uses the same diffusion theory routine as DIFF 2D and is able to perform overall burn-up calculations in two dimensions. Cross sections are derived from interpolation in tables generated by CDB.

The SYNTRON program[7, 20] is a 3-dimensional flux synthesis program using 2-dimensional trial functions produced in the program by a routine which is very similar to DIFF 2D. In not too complicated cases two trial functions are used, and axial mixing functions are found by an iterative scheme.

Both diffusion theory programs usually work with 2-group cross sections produced by CDB.

In addition to the usual boundary conditions Y-matrices can be used. These are produced by HECS[21] which by means of collision probability methods in slab or cylindrical geometry calculates the linear relationship on a suitable surface between the current in each group and the fluxes in all groups. The cross sections used in HECS are generated by the CRS program.

2.7. Adjustments and Fitting

The primary object with the cross section generating system has been the making of reliable calculations on light-water reactors. However, no special effort to fit the data for this purpose has been made so far, except for a certain ad hoc correction[22] of the resonance absorption of ^{238}U, which will, as is well known, be too high if based exclusively on differential data.

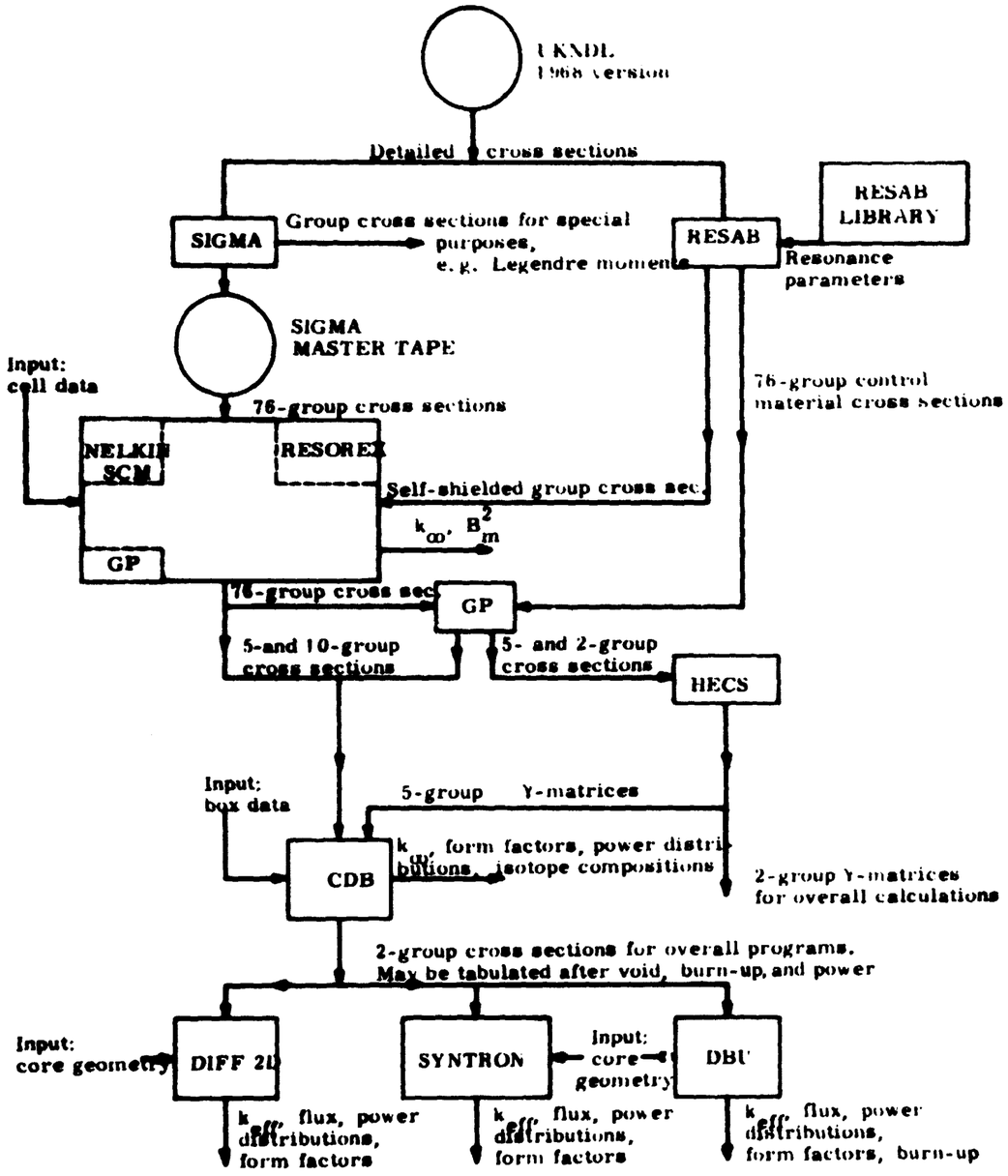

Fig. 2.a. Parts of the Risø reactor physics code system used in the CY calculations.

3. DESCRIPTION OF THE CONNECTICUT YANKEE REACTOR

The Connecticut Yankee reactor is a pressurized-water reactor with a present licensed thermal power level of 1825 MW_{th} (600 MW gross electrical) increased from 1473 MW_{th} (490 MW gross electrical) in March 1969. Core loading started on 1 July 1967, and criticality was first achieved on 24 July in the fully loaded core. The plant is located near Haddam, Connecticut, U.S.A., on the east bank of the Connecticut River.

The reactor plant and the turbine generator and various auxiliary equipment were designed and supplied by the Westinghouse Electric Corporation. The Stone and Webster Engineering Corporation was responsible for site development, design of buildings, secondary systems, and plant constructions. Below follows a short description of reactor components and characteristics of interest in connection with the calculations described in the present report. For detailed plant descriptions, reference is made to the CY Facility Description and Safety Analysis[1].

3.1. Reactor Core

The reactor core approximates a circular cylinder with an equivalent diameter of about 127 inches and an active height of 122 inches. It is made up of 32028 SS304 clad fuel rods containing 74.8 metric tons of slightly enriched uranium in the form of pressed and sintered UO_2 pellets. The fuel rods are located on a square pitch in a 15x15 array to make a fuel assembly. Some of the fuel rods are omitted to allow installation of 20 control rod guide tubes which accept the movable control rod clusters. In addition the central fuel rod is omitted from each assembly, resulting in a total of 204 fuel rods per element (fig. 3.1.a). The fuel element (shown in figs. 4.1-2 of ref. 1) is of the canless type. The control rod guide thimbles and the instrumentation thimble constitute the basic assembly. The construction of a fuel element is the same whether or not a rod cluster control assembly will be utilized, as the main support structure of the element is in both cases obtained by welding the twenty rod cluster control guide tubes to seven Inconel-718 grids and to the top and bottom nozzles. The fuel rods are supported laterally by the Inconel spring clips of the grid assemblies in such a way that each fuel rod is free to expand and contract both axially and radially without bending, as its temperature changes.

The core contains 157 fuel elements divided into three concentric regions of 3.00, 3.24, and 3.67 w% ^{235}U enriched uranium. The inner

region consists of 53 fuel elements at 3.00 w% ^{235}U and the two outer regions contain 52 fuel elements each (3.24 w% and 3.67 w%) as shown in fig. 3.1.b.

When the core is refuelled, spent fuel will be removed from the central region of the core. Fuel from the intermediate and outer regions will be moved inward, and fresh fuel (enrichment 3.67% at the first refuelling - otherwise 4%) is loaded in the outer region.

3.2. Reactivity Control

The control system consists of 45 rod clusters, each cluster containing 20 control rods made of a silver/indium/cadmium alloy sealed in stainless steel (SS304). This alloy is almost black to thermal neutrons and has a resonance absorption that significantly increases its reactivity worth.

As seen from fig. 3.2.a the control rod clusters are divided into four groups, two control groups (A and B) and two shutdown groups (C and D). The control groups are partly inserted in the core at power and are used to compensate for reactivity changes associated with changes in operating conditions. The reactivity controlling values of the four groups are approximately (Hot Zero Power condition):

A: 2.7% ∂k/k

B: 1.8% ∂k/k

C: 2.0% ∂k/k

D: 1.1% ∂k/k

Reactivity control is provided by the control rods described above and by a soluble chemical neutron absorber (in the form of boron acid) in the reactor coolant/moderator. The concentration of the boron is varied from about 0 to 2500 ppm during the core life in order to compensate for changes in reactivity arising from changes in the coolant temperature from cold to Hot Zero Power (HZP) conditions and changes originating from fission product poisons (including Xe and Sm) and losses due to fuel burn-up. The control rods are used for shutdown, reactivity changes caused by programmed increase in the average coolant temperature above the HZP temperature, and reactivity changes occurring as a result of the power coefficient of the reactor.

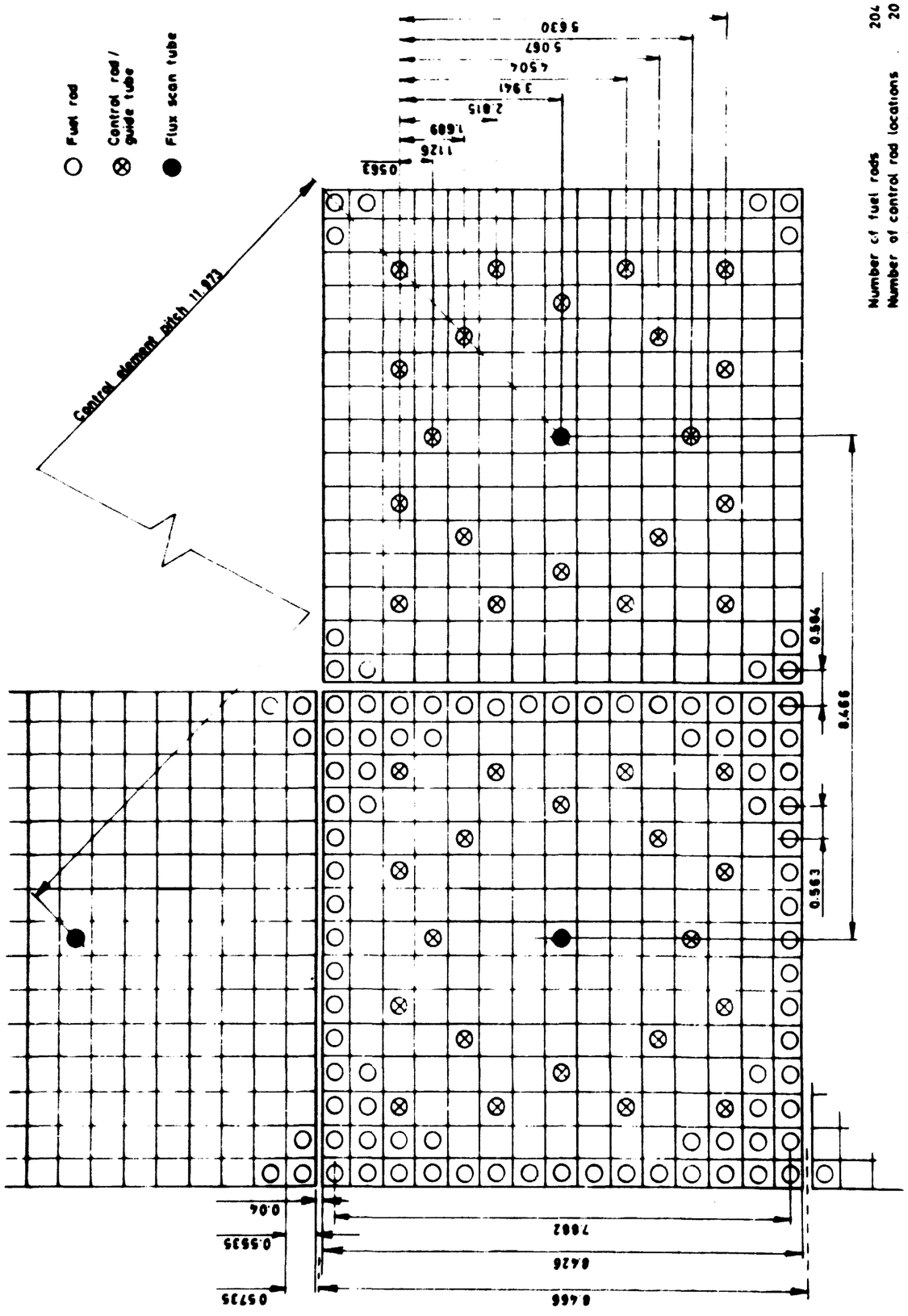

Number of fuel rods 204
Number of control rod locations 20
Number of flux scan positions 1

Fig. 3.1.a. Geometrical box data (inches). Cold dimensions.

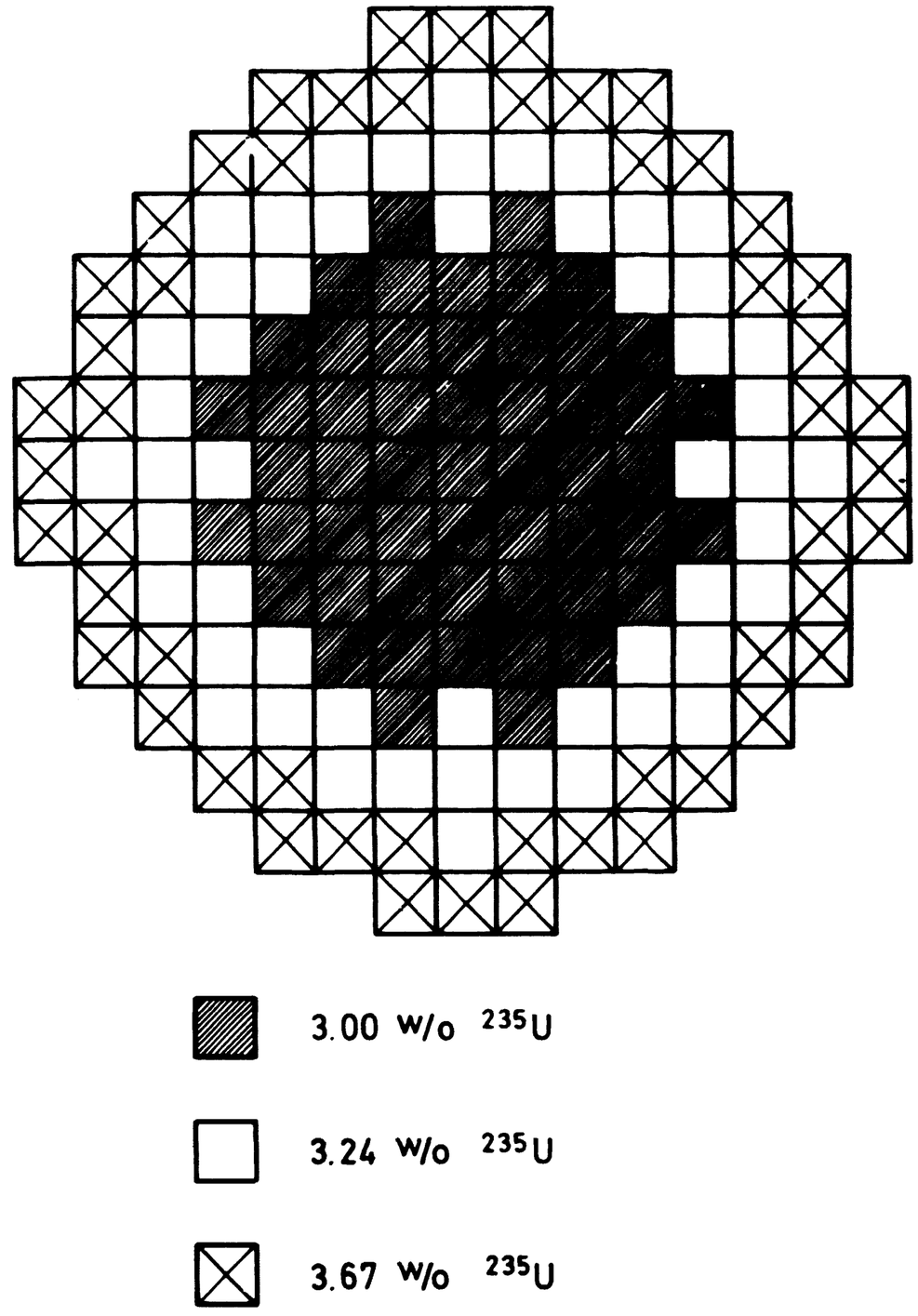

Fig. 3.1.b. Connecticut Yankee. Enrichment boundaries in the first cycle.

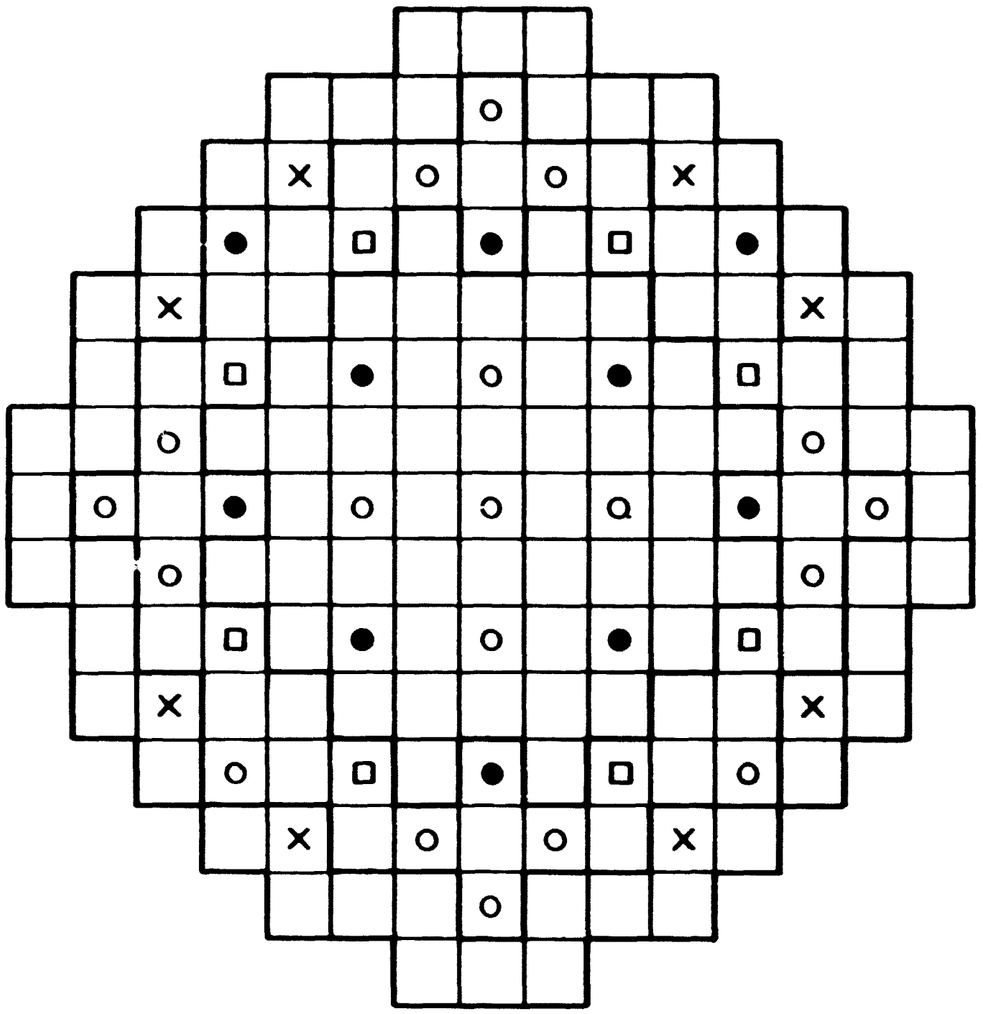

● Cluster in control group B (12 clusters)

○ Cluster in control group A (17 clusters)

□ Shutdown control cluster, group C (8 clusters)

× Shutdown control cluster, group D (8 clusters)

Fig. 3.2.a. Connecticut Yankee. Subdivision of control clusters.

4. CY CORE CHARACTERISTICS

A selection of data for the CY reactor has been compiled and prepared[23]. Some of the data are presented in this report. On the basis of the fundamental data[1-5] quoted below, the number densities and dimensions given in tables 4.1.a - 4.1.c were calculated.

4.1. Fundamental Data

a) Asymptotic fuel cell, geometrical data, 20°C dimensions, inches:

Outside diameter of SS-clad tube	0.422
SS-clad thickness	0.0165
Diametric gap	0.0055
Pellet diameter	0.3835
Rod pitch (square)	0.563
Active fuel length	121.8

b) Temperatures used in calculations of hot dimensions, °F:

Zero power		255
Hot zero power		550
Hot full power	fuel, av.	1355
	clad, av.	605
	mod., av.	568

c) Pressures used in calculations of number densities of boron and moderator, psia:

Zero power	425
Hot zero and full power	2165

d) UO_2 densities, 20°C, g/cm³:

3.00 w% ^{235}U	10.30
3.24 w% ^{235}U	10.30
3.67 w% ^{235}U	10.19

e) Cladding material: SS304. Composition: 19% Cr, 10% Ni, 71% Fe (standard composition[24]). Density[1-2]: 0.289 lb/in^3.

f) Coolant/moderator material: H_2O.

H_2O densities as functions of temperature and pressure were calculated from the data given in ref. 25.

g) Boron-10, measured concentration[5]: 19.5% $\pm$ 0.5% (atom per cent).

h) Control cell. Guide tube and cladding material: SS304. Control rod material: Ag/In/Cd, density: 10.22 g/cm^3 [26].
Dimensions, 20°C, inches:

Inside diameter of guide tube	0.519
Thickness of guide tube	0.012
Radial gap	0.0395
Outer diameter of SS-clad tube	0.440
SS-clad thickness	0.0195
Diametric gap	0.0035
Control rod diameter	0.3975

i) Inconel. Material specification: In 718.

Composition: 0.04% C, 19% Cr, 18% Fe, 0.6% Al, 0.8% Ti, 5% Nb, 3% Mo, 53.56% Ni (standard composition of In 718 - ref. 12)

Density: 0.297 lb/in^3 (refs. 1, 2)

Total weight of Inconel in core: 1800 lbs.

j) Overall dimensions, 20°C, inches:

Max. core width 15 x 8.466	126.99
Max. inside baffle width	127.02
Thickness of baffle	0.50
Core barrel inner diameter	131.25
Thickness of barrel	1.78
Thermal shield inner diameter	137.60
Thermal shield thickness	4.00

Pressure vessel inner diameter	154.00
Pressure vessel thickness	11.00

As mentioned earlier the data presented formed the basis of the calculation of data given in tables 4.1.a-c.

Table 4.1.a

Asymptotic fuel cell data

		Cold	Zero power	Hot zero power	Hot full power
		Temperature (°C)			
Fuel		20	124	288	735
Cladding		20	124	288	318
Moderator		20	124	288	298
		Dimensions (cm)			
Outside rad. of fuel pellet		0.487045	0.487447	0.488082	0.489810
Eq. outside rad. of gap		0.494030	0.494944	0.496383	0.496646
Outside rad. of SS-clad tube		0.535940	0.536931	0.538492	0.538778
Eq. rad. of fuel cell		0.806802	0.808293	0.810645	0.810788
		Number density (10^{24} At/cm^3)			
Cladding	Cr	0.0176031	0.0175059	0.0173540	0.0173264
	Ni	0.00820747	0.00816214	0.00809132	0.00807845
	Fe	0.0612574	0.0609190	0.0603905	0.0602944

Table 4.1.b

Fuel cell data

Gap and cladding homogenized, Inconel included in cladding, box water gap included in eq. radius of the fuel cell

		Cold	Zero power	Hot zero power	Hot full power
		Dimensions (cm)			
Outside rad. of fuel pellet		0.487045	0.487447	0.488082	0.489810
Outside rad. of SS-clad tube		0.535940	0.536931	0.538492	0.538778
Eq. outside rad. of fuel cell		0.808809	0.810303	0.812660	0.812804
		Number density (10^{24} At/cm^3)			
Region I	^{235}U	0.000697983	0.000696257	0.000693546	0.000686229
Enrichment:	^{238}U	0.0222830	0.0222279	0.0221414	0.0219078
3.00 w/o ^{235}U	O	0.0459620	0.0458483	0.0456698	0.0451880
Region II	^{235}U	0.00075381	0.000751955	0.000749027	0.000741125
Enrichment:	^{238}U	0.0222278	0.0221728	0.0220865	0.0218535
3.24 w/o ^{235}U	O	0.0459635	0.0458496	0.0456711	0.0451893
Region III	^{235}U	0.000844738	0.000842649	0.000839368	0.000830513
Enrichment:	^{238}U	0.0218926	0.0218384	0.0217534	0.0215239
3.67 w/o ^{235}U	O	0.0454746	0.0453621	0.0451855	0.0447088
Cladding, no Mn.	N_{Cr}	0.0168918	0.0168002	0.0166572	0.0166256
	N_{Ni}	0.00998805	0.00993593	0.00985429	0.00982995
	N_{Fe}	0.0538828	0.0535862	0.0531229	0.0530354
Cladding, 1.76% Mn.	N_{Cr}	0.0168918	0.0168002	0.0166572	0.0166256
	N_{Ni}	0.00998805	0.00993593	0.00985429	0.00982995
	N_{Fe}	0.0525873	0.0522978	0.0518456	0.0517602
	N_{Mn}	0.00131702	0.00130974	0.00129838	0.00129631
Coolant/ moderator	N_H	0.0667520	0.0627729	0.0500931	0.0487852
	N_O	0.0333760	0.0313864	0.0250466	0.0243926
	N_B10 /(ppm x 10^{-6})	0.0108413	0.0101950	0.00813569	0.00792327
	N_B11 /(ppm x 10^{-6})	0.0447550	0.0420871	0.0335858	0.0327089

Table 4.1.c

Control cell data

	Cold	Zero power	Hot zero power	Full power
	Dimensions (cm)			
Ag-In-Cd control rod rad.	0.504825	0.505907	0.507613	0.507717
Eq. outside rad. of gap	0.509270	0.510211	0.511695	0.511786
Outside rad. of SS-clad tube	0.558800	0.559833	0.561461	0.561561
Eq. outside rad. of gap	0.659130	0.660348	0.662269	0.662386
Outside rad. of guide tube	0.689610	0.690884	0.692894	0.693017
Eq. rad. of fuel cell	0.806802	0.808293	0.810645	0.810788
Eq. cell rad. incl. box water gap	0.808809	0.810303	0.812660	0.812804
	Number densities (10^{24} At/cm^3)			
N_{Ag}	0.0456492	0.0453569	0.449010	0.0448734
N_{In}	0.00804187	0.00799038	0.00791007	0.00790521
N_{Cd}	0.00273808	0.00272055	0.00269320	0.00269155

5. CRITICALITY CALCULATIONS

As a first verification a calculation of the effective multiplication factor for the reactor condition ZERO POWER (ZP) with a coolant boron concentration of 2040 ppm was carried out. According to ref. 4 this boron concentration corresponds to the "All Rods Out" critical condition for a clean core at 260°F, (pressure 435 psig).

The basic cross sections used in the calculations were obtained from the SIGMA MASTER TAPE. Briefly described the calculations consisted of the following steps:

1. Condensation to 10-group microscopic cross sections for unit fuel cells with the enrichments 3.00, 3.24, and 3.69%. The fuel cell data used in the calculations were obtained from table 4.1.b, which means that the fuel/cladding gap and the cladding were homogenized. Furthermore the Inconel grids were assumed to be homogeneously distributed in the cladding material without affecting the cladding volume, (CRS).

2. Condensation to 5-group macroscopic cross sections for water-filled control rod guide tubes surrounded by a water layer. In the calculations this geometry was surrounded by a homogenized fuel cell layer, (CRS + GP).

3. Generation of 2-group cross sections for fuel elements of different enrichments based on the cross sections from points 1 and 2, (CDB).

4. Condensation of 76-group cross sections to 2-group cross sections for core baffle and the reflector composed of alternating layers of stainless steel and boron poisoned water, (CRS + GP).

5. On the basis of the 2-group cross sections from points 3 and 4 an overall two-dimensional calculation of k_{eff} was performed. The core baffle was explicitly represented in the calculations (previous experience from Yankee Rowe burn-up calculations - ref. 9). A total of 71 x 71 mesh was used in the calculations on a quarter of the core, (DIFF 2D).

Details on the core geometry representation and mesh structures used in the calculations are given in ref. 27.

No information was available on the Mn content in the SS304 used in CY, but analyses of SS304 reported elsewhere seem to show Mn contents of 1.6-1.8%. A Mn content of 1.74% was chosen in accordance with ref. 28.

The result of the criticality calculations described above was

$k_{eff} = 1.0058$.

There can be a lot of reasons for the deviation (0.58%) from unity, and no special effort was made to investigate them. The uncertainty in the stainless steel SS304 (standard composition) results e.g. in a variation in k_{eff} of more than 0.5% ∂k/k. As an example it can be mentioned that calculations showed a variation in k_{eff} of 0.41% ∂k/k per % Mn in the cladding.

The effect of a few approximations in the calculations was, however, investigated. In the first step in the calculations (CRS), the fuel cell was homogenized before the spectrum calculations. This approximation introduced an error of only 1 o/oo ∂k/k and correspondingly small errors in the isotope concentrations during burn-up.

Calculations on the HZP condition of the reactor showed that the overall 2-group representation was sufficient. A comparison between an overall 2-group and a 5-group calculation showed no difference in the value of k_{eff} to four decimals.

6. CONTROL ROD WORTH. DIFFERENTIAL AND INTEGRAL VALUES

The reactivity worth of different control rod groups was calculated using three-dimensional diffusion theory.

For these calculations homogenized 2-group cross sections have to be produced for the fuel boxes with and without control rods inserted.

The generation of cross sections for the unrodded fuel boxes, core baffle, and the reflector has already been described.

Cross sections for the control material consisting of a silver-indium-cadmium alloy pose special problems because of the strong resonance character of the absorption in these components.

6.1. Calculation of CDB Cross Sections for Control Rod Cells

The calculations are carried out in the following steps.

First the Dancoff factor for a control rod super cell inside the smallest dotted square indicated in fig. 6.1.a is calculated. Apart from the control cell with control rod, cladding guide tube and associated moderator, the super cell contains fuel, cladding, and moderator from a total of 3 fuel elements. Dimensions and densities are taken from table 4.1.c.

The super cell is transformed into an equivalent cylinder as shown in fig. 6.1.b. The fuel is arranged as an outer annulus with the cross section Σ_f^c.

The annular region between the fuel and control rod contains the homogenized moderator present in the super cell, yielding the cross section Σ_m^s, and into the same region the stainless steel from fuel and control rod cladding as well as from the guide tube is homogenized, giving the cross section Σ_m^c.

The cross sections Σ_f^c, Σ_m^s, and Σ_m^c are based on the potential scattering cross section of the fuel, the moderator, and the stainless steel respectively.

From these cross sections and the geometry of the equivalent cylinder cell the Dancoff factor, dc, for the control rod is calculated with the assumption that the nuclides in fuel and cladding are infinitely heavy. This assumption is reasonable because the main part of the control absorption is due to broad resonances at low neutron energy.

The calculations are carried out in a small program, CRDC, using the formulas derived in the Appendix.

The control rod contains four different types of resonance absorbers,

Ag, In, Cd_0, and $Cd_{1/2}$, the two last-mentioned nuclides with spin 0 and 1/2 have to be treated separately because of the difference in spin.

For each absorber a value, S, of the effective excess scattering cross section per absorber nuclide is calculated by CRDC according to the formula:

$$S = a/(2 \times R_c \times N_{abs}),$$

where R_c is the radius of the control rod and N_{abs} the atom density in the rod of the absorber in question. The quantity a is calculated according to formulas 2.2 and 3.1.2 in ref. 19.

For each absorber a quantity PSHET, which is the total slowing down power in the super cell per atom of the absorber in question, is calculated.

For each absorber nuclide 76-group cross sections are calculated in RESAP Resonance parameters from the RESAB library are used in this calculation, which is performed by the semianalytical LINK ALFA method with S and PSHET as parameters except for the strong low energy resonances, which are calculated in exact slowing down theory, involving a large number of fine groups.

The individual absorber cross sections are then combined into a macroscopic 76-group cross section set for the control rod.

This procedure is justified where no significant interaction takes place between the resonances of the fuel and the control absorbers and between the resonances of the individual control absorber nuclides.

A new super cell is set up inside the large dotted square in fig. 6.1.a containing now the control cell and its eight nearest neighbouring fuel pin cells.

In fig. 6.1.c an equivalent cylinder representation is shown, where the eight fuel pin cells are homogenized into the cross-hatched area surrounding the control rod cell.

76-group cross sections for the remaining materials, i.e. homogenized fuel pin cell material, moderator, and cladding, are provided by CRS.

The 76-group flux in the super cell is calculated by the program GP and used to produce homogenized and condensed 5-group cross sections for the control rod cell for use in the CDB fuel box code. Finally the CDB code produces homogenized 2-group cross sections for the control rod bearing fuel boxes.

6.2. Overall Calculations

A detailed mesh structure of two horizontal cuts through the reactor, very similar to the one used in the earlier described overall calculations in two dimensions, was set up for the SYNTRON calculations.

In those calculations two trial functions were generated, one in a horizontal cut with the movable control rods out, and one with the rods present.

A first SYNTRON calculation of the reactivity worth of control group A with group B present in the core (see fig. 3.2.a) gave very poor results as compared with the experimental value.

It is assumed that the reason for this is the restriction on mesh points imposed by SYNTRON.

A two-dimensional calculation using 50 x 50 mesh points as compared with 39 x 39 mesh points in SYNTRON gave improved results.

In order to save meshes the core baffle and reflector were replaced by a boundary condition in the form of a Y-matrix.

Detailed 2-group cross sections for the various layers of steel and water constituting the reflector and core baffle already existed, and it was possible with the program HECS to calculate a 2-group Y-matrix corresponding to a detailed slab geometry representation of core baffle and reflector.

The effect of the introduction of this Y-matrix was rather spectacular as summarized in the following.

		Total reactivity worth, $\partial k/k$, for control rod group A
1.	Measured value	0.0274
2.	DIDD 2D, 2-dimensional Full reflector, 50 x 50 mesh	0.0256
3.	SYNTRON Full reflector, 39 x 39 -	0.0366
4.	DIFF 2D, 2-dimensional Y-matrix, 45 x 45 -	0.0268
5.	SYNTRON Y-matrix, 23 x 23 -	0.0266
6.	SYNTRON Y-matrix, 38 x 38 -	0.0274
7.	SYNTRON Y-matrix, 45 x 45 -	0.0276

It is seen that even a rather coarse mesh combined with Y-matrix gives an acceptable result. This indicates that the real trouble is that of obtaining a sufficiently fine subdivision in the rather complicated region outside the core.

6.3. Results

As a reasonable compromise between accuracy and computing speed the remaining calculations with SYNTRON were carried out with Y-matrix in combination with 38 x 38 mesh points.

The following results were obtained:

Control rod group	Total reactivity worth ∂k/k	
	Measured[5]	Calculated
A	0.0274	0.0274
B	0.0180	0.0202
D	0.0110	0.0112

In figs. 6.4.a and 6.4.b are shown curves for the differential and integral control rod values respectively for group A with group B in core, and for group D with groups A and B in core.

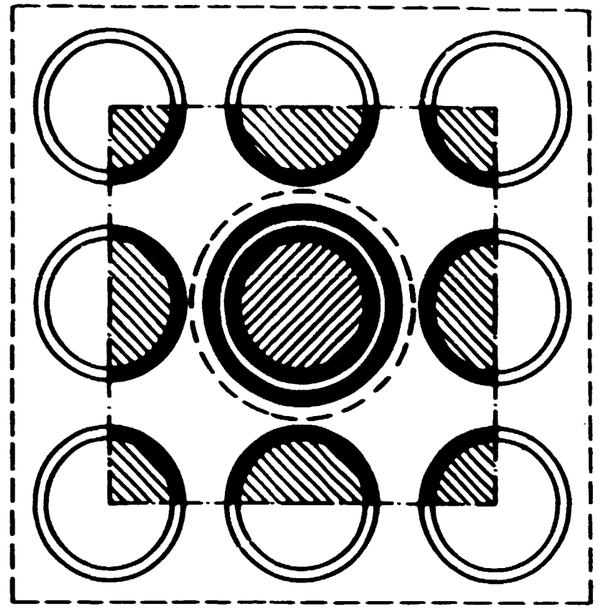

Fig. 6.1.a. Dancoff factor calculation. Control rod super cell.

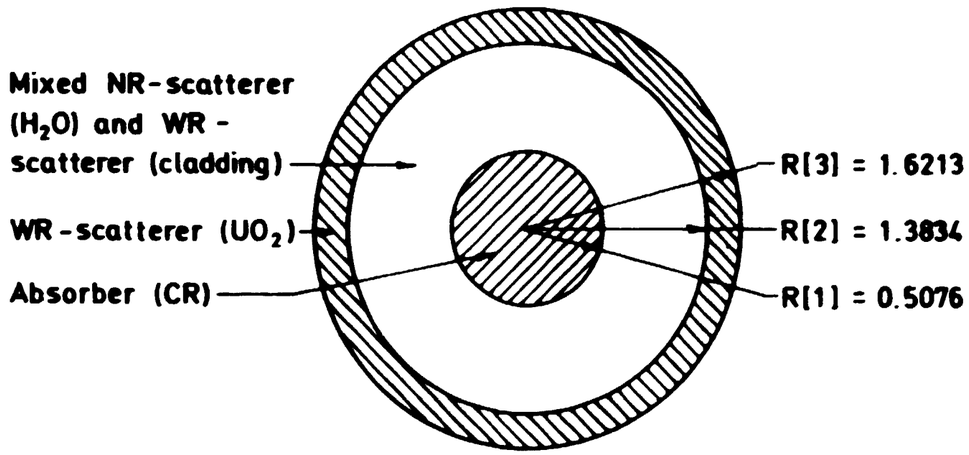

Fig. 6.1.b. Dancoff factor calculation. Equivalent cylinder.

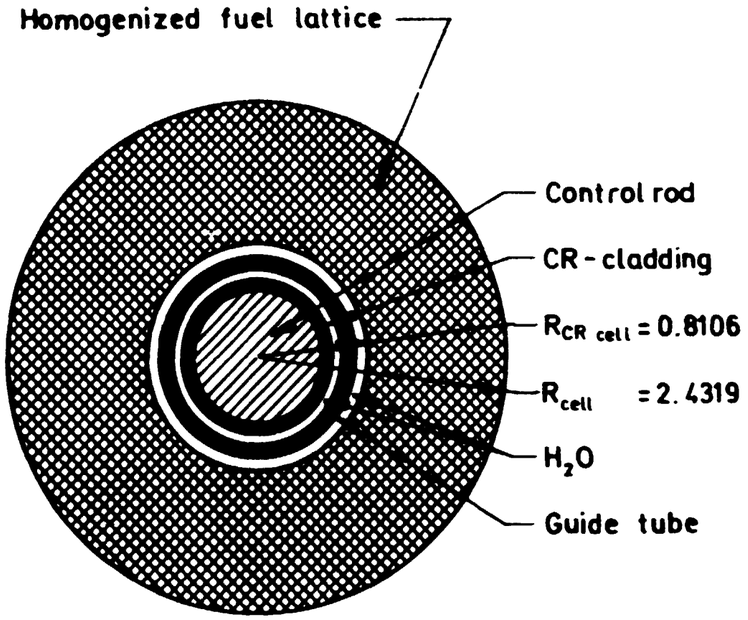

Fig. 6.1.c. Super cell geometry used to produce homogenized and condensed 5-group cross sections.

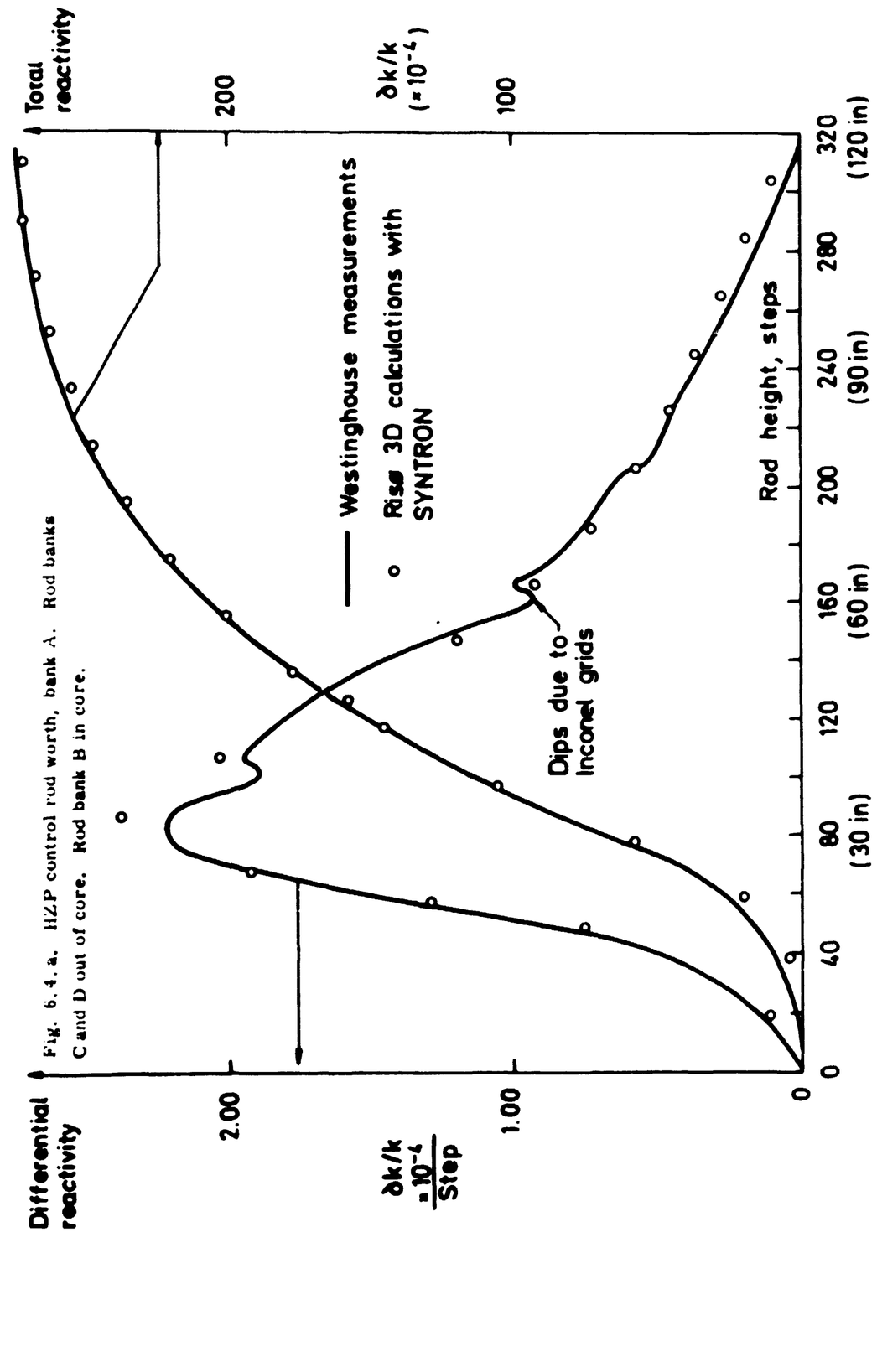

Fig. 6.4.a. HZP control rod worth, bank A. Rod banks C and D out of core. Rod bank B in core.

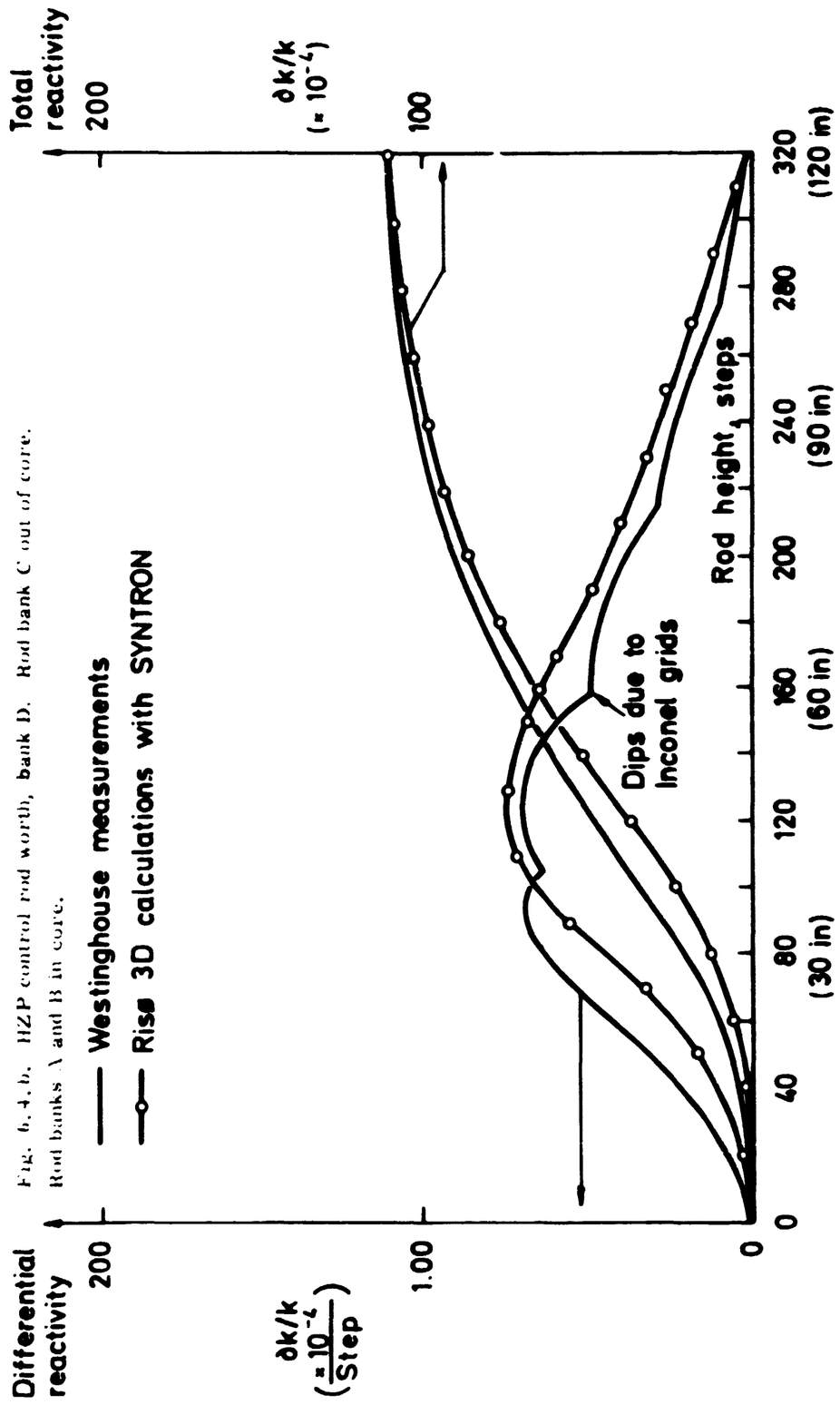

Fig. 6.4.b. HZP control rod worth, Rod banks A and B in core.

7. CALCULATIONS OF REACTIVITY AND POISON COEFFICIENTS

7.1. Calculation of Moderator Temperature Coefficients. No Spectrum Effects Included

In the first series of calculations of the moderator temperature coefficients, $\frac{\partial k}{k}/\partial t$, at the reactor condition HZP, the spectrum variation in the condensed 10-group microscopic cross sections arising from a variation in the temperature of $\pm$ 10°C ($\pm$ 18°F) from the nominal temperature 288°C (1550°F) was not taken into account. Only the density effect was considered. The calculations were performed with boron concentrations of 1500, 2000, and 2500 ppm. The necessary data were obtained from ref. 23. The calculations were carried out at the "All Rods Out" condition.

As no spectrum effects were included, the 278° and 298°C cross sections used in CDB were obtained by changing the density of the moderator (H, O, ^{10}B, and ^{11}B).

The calculations at the three temperatures (288° and 288° $\pm$ 10°C) followed the steps described in chapter 5.

Box values (5-group calculations) and overall calculations (2-group calculations) of the moderator temperature coefficients are shown in fig. 7.1.a.

Fig. 7.1.b shows a comparison between Risø overall 2D-calculations of the moderator temperature coefficient and the Westinghouse 1D-calculations with LEOPARD and AIM5 (ref. 2). The same figure shows the results of measurements for different reactor conditions. As will be seen it is difficult to compare measurements and calculations because the calculation condition is an "All Rods Out" fresh core. The measured "All Rods Out" curve corresponds to different levels of core burn-up, while the "fresh" curve corresponds to control groups partly inserted in the core. The positions of the control rod groups are specified in ref. 5.

7.2. 2000 ppm Moderator Temperature Coefficient. Spectrum Effects Included

For an estimate of the importance of the spectrum effects, the next series of calculations covered calculations of the moderator temperature coefficient at a concentration of 2000 ppm, taking spectrum effects into account. This means that the microscopic 10-group cross sections for the fuel cells of different enrichments had to be calculated with CRS at the temperatures 278, 288, and 298°C, keeping the fuel temperature at 288°C.

As seen from fig. 7.1.a the value of the coefficient increased from 0.62 x 10^{-4} to 0.69 x 10^{-4} $\frac{\partial k}{k}/\partial t$ ($^{o}F^{-1}$).

7.3. Leakage Dependence of the Moderator Temperature Coefficients

From fig. 7.1.a it is seen that the neutron leakage plays an important role for the value of the temperature coefficients. For this reason a third series of calculations was carried out (2000 ppm, spectrum effects included) where the number of groups in the overall calculations was raised from 2 to 5. As seen from the figure this introduced only a minimal variation in the coefficient.

7.4. Doppler Coefficients

The Doppler coefficient defined as the change in reactivity per degree of the effective fuel temperature[2] is shown in fig. 7.4.a. The Westinghouse spectrum calculation results were obtained with LEOPARD[2]. The Risø calculations were carried out using CRS/GP/CDB/DIFF 2D. Calculations showed - as expected - that the difference between CRS values of the Doppler coefficient and the coefficients using CRS/GP/CDB/DIFF 2D was minimal. As seen from the figure a single value of the coefficient was calculated, using the more exact RESAB code.

7.5. Poison Coefficients

Fig. 7.5.a shows the results of Risø calculations of reactor coolant boron worth, - $\frac{\partial k}{k}/\partial$ppm, versus boron concentration at start of life. The same figure shows the Westinghouse calculations and measurements of the same quantity. These measurements were made in conjunction with control rod bank worth measurements so that a reactor coolant dilution or boration was maintained while a control rod bank was inserted or withdrawn to sustain criticality. An inherent difference exists between the measured and the calculated worth curves on account of the methods by which the worth is obtained. The measurements necessitate rod banks to be in core and changing in height over the measurements, while all calculations are "All Rods Out" calculations.

DBU uses tabulated cross sections calculated with CDB, tabulated as functions of initial enrichments, burn-up, and power densities. During the DBU burn-up calculations the reactor is held critical by poison cross sections. Different poison cross sections may be used in the different regions of the reactor, and criticality is maintained by multiplying all poison cross

sections by an eigenvalue parameter α. If poison coefficients ($\partial\Sigma_a^B/\partial$ppm) are used in the different regions, the critical α-value at a certain burn-up level is identical with the critical coolant boron concentration. This means that the poison coefficients must in principle be known as functions of initial enrichment, burn-up, and boron concentration levels.

As described in chapter 8 three different types of burn-up calculations were carried out on the first CY core loading in order to investigate how detailed the specification of the poison coefficients should be for satisfactory results to be obtained:

a) Constant values (independent of enrichment, burn-up, etc.) of the poison coefficients specified in two energy groups:

$\partial\Sigma_{a1}^B/\partial$ppm = 1.25 x 10^{-7}, $\partial\Sigma_{a2}^B/\partial$ppm = 7.2 x 10^{-6}.

b) $\partial\Sigma_{a1}^B/\partial$ppm = 1.25 x 10^{-7}, $\partial\Sigma_{a2}^B/\partial$ppm = f (initial enrichment, burn-up).

c) $\partial\Sigma_{a1}^B/\partial$ppm = 1.25 x 10^{-7}, $\partial\Sigma_{a2}^B/\partial$ppm = f (initial enrichment, burn-up, ppm concentration level).

The value of $\partial\Sigma_{a2}^B/\partial$ppm used in cases b and c was obtained from fig. 7.5.b, Risø calculations of HFP values of poison coefficients versus ppm concentration, enrichment, and burn-up. The values of $\partial\Sigma_{a2}^B/\partial$ppm as used in the DBU calculations, case b, - obtained from fig. 7.5.b assuming a linear dependence - are shown in fig. 7.5.c. Similarly the coefficients used in the DBU calculations, case c, are given in figs. 7.5.d-e. Two ppm poison levels (500 and 1500 ppm) were used.

Detailed information on the CRS/GP/CDB calculations of the coefficients is given in ref. 29. As a general remark it should be mentioned that investigations showed that the coefficients could be calculated without taking into account the spectrum variation arising during burn-up, which means that the CRS microscopic group cross sections used in CDB were calculated with densities corresponding to BU = 0.

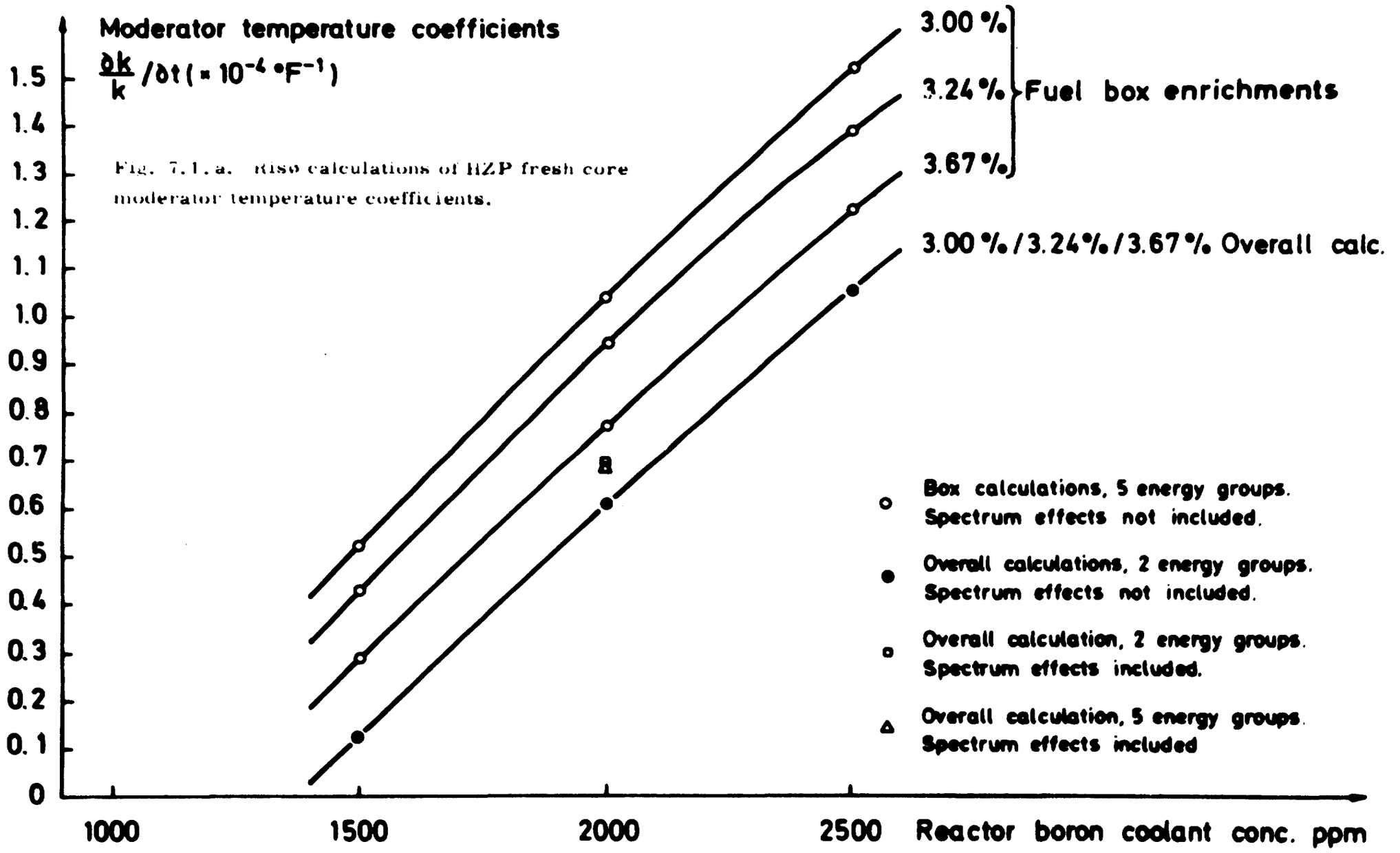

Fig. 7.1.a. Rise calculations of HZP fresh core moderator temperature coefficients.

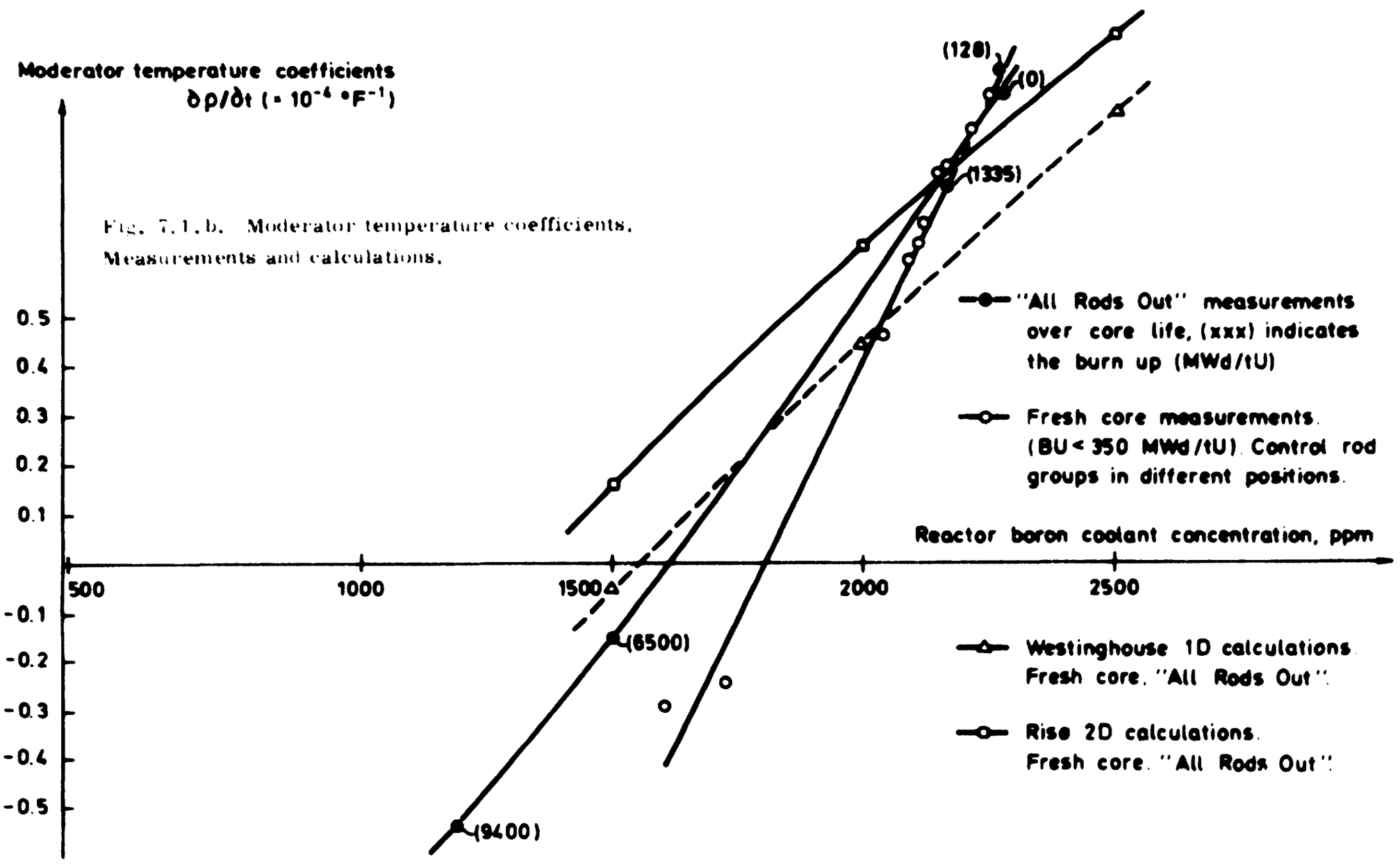

Fig. 7.1.b. Moderator temperature coefficients. Measurements and calculations.

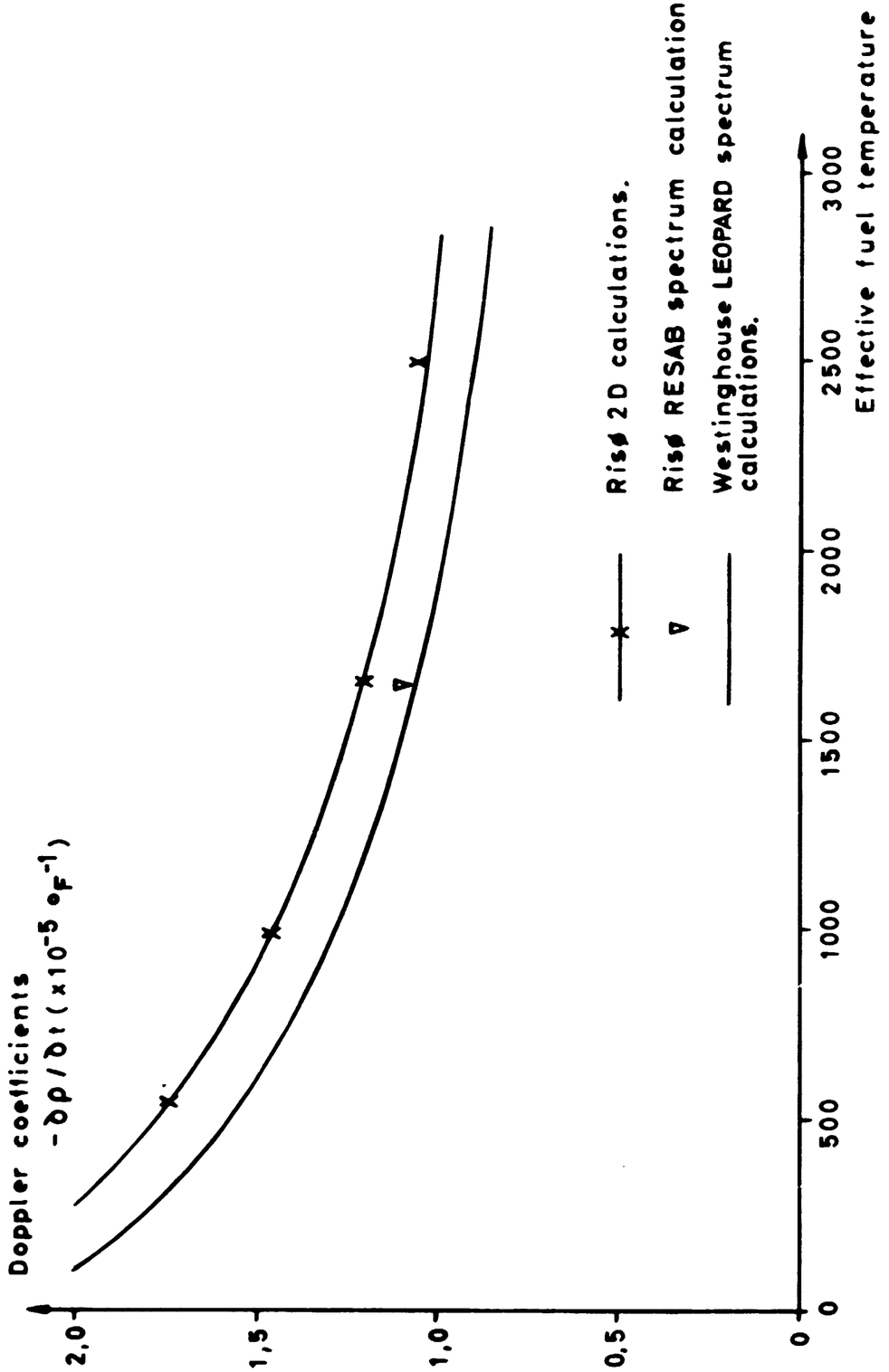

Fig. 7.4.a. Doppler coefficients versus effective fuel temperature.

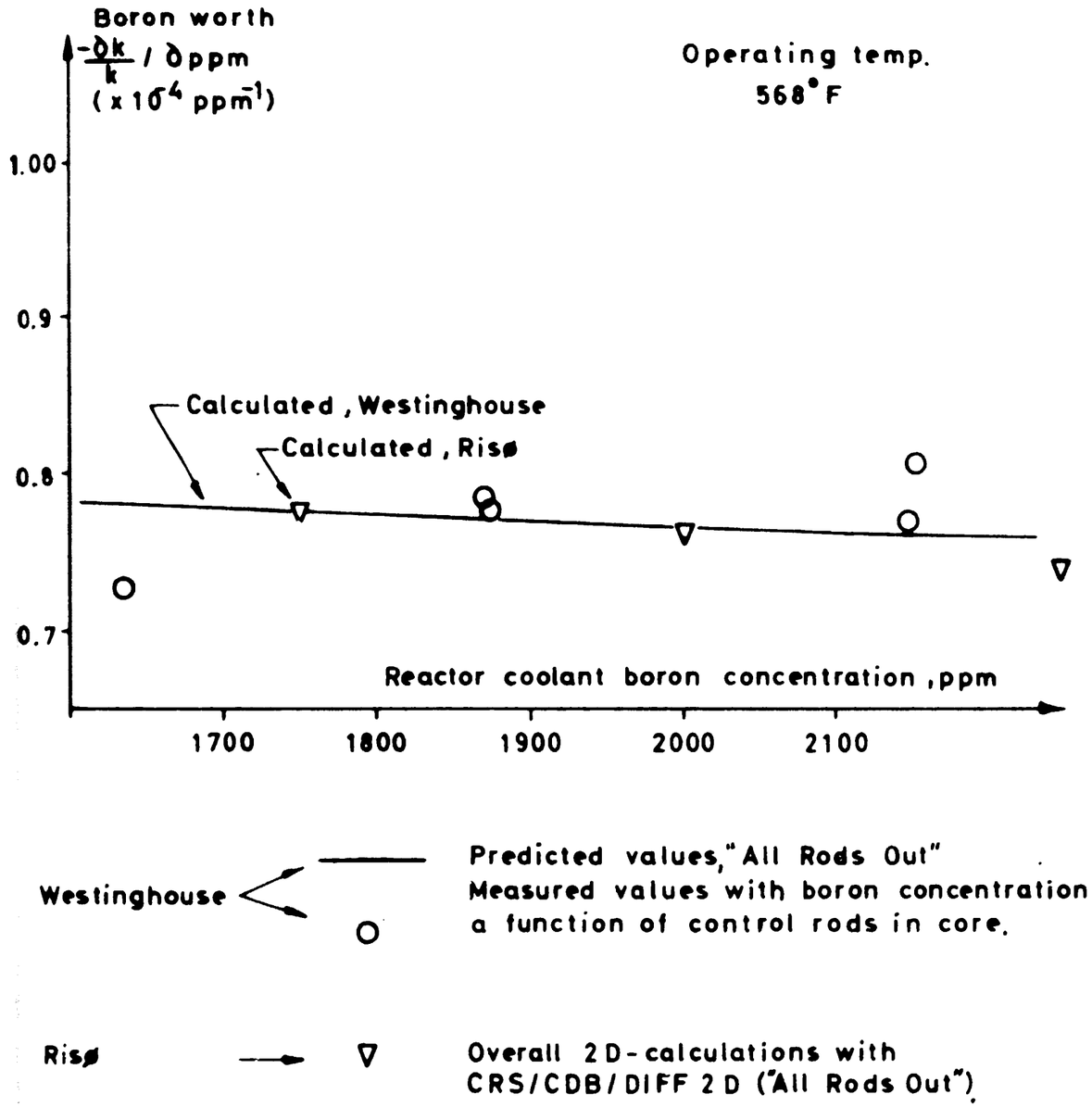

Fig. 7.5.a. Reactor coolant boron worth versus boron concentration at start of life.

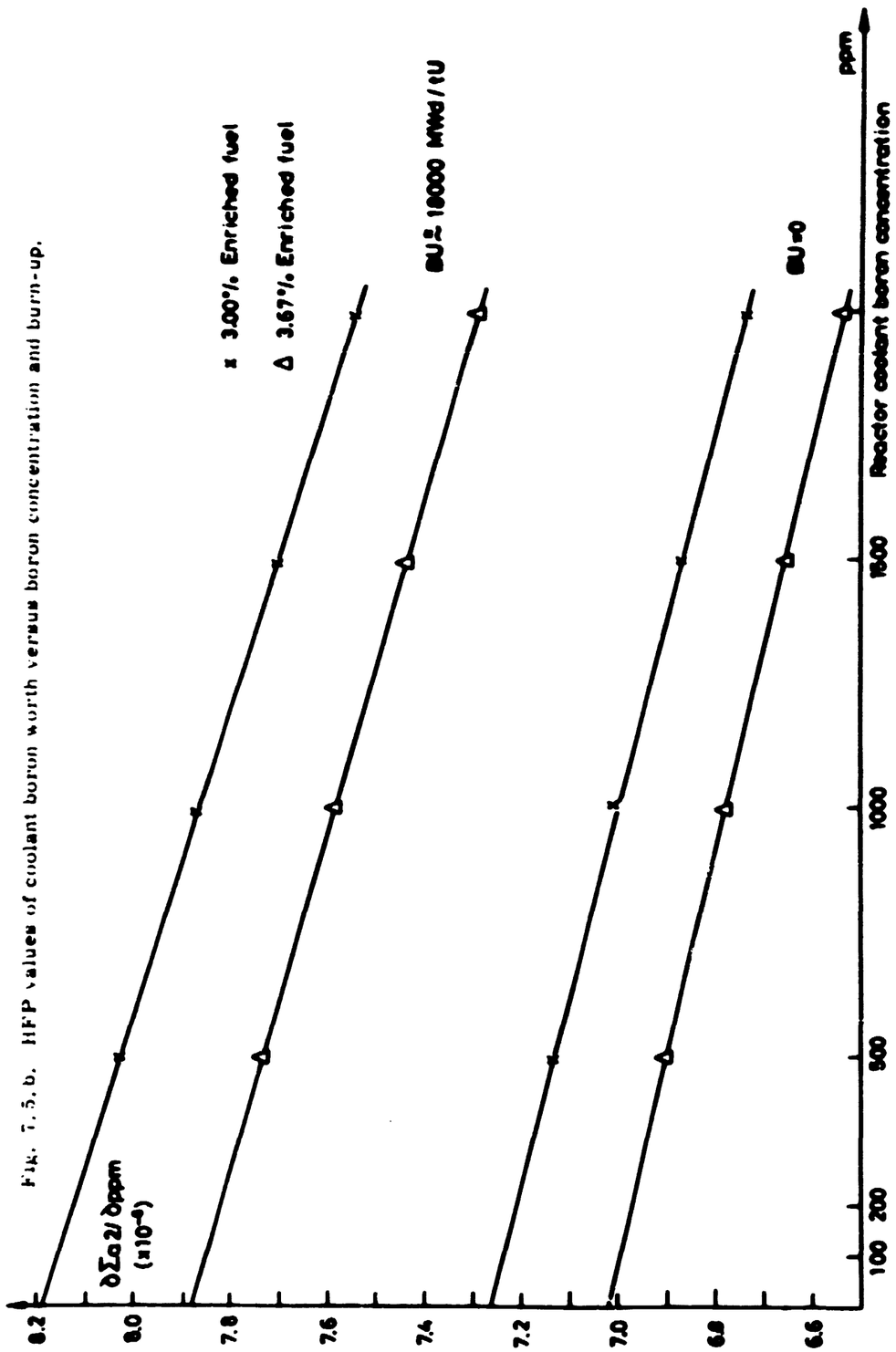

Fig. 7.5.b. HFP values of coolant boron worth versus boron concentration and burn-up.

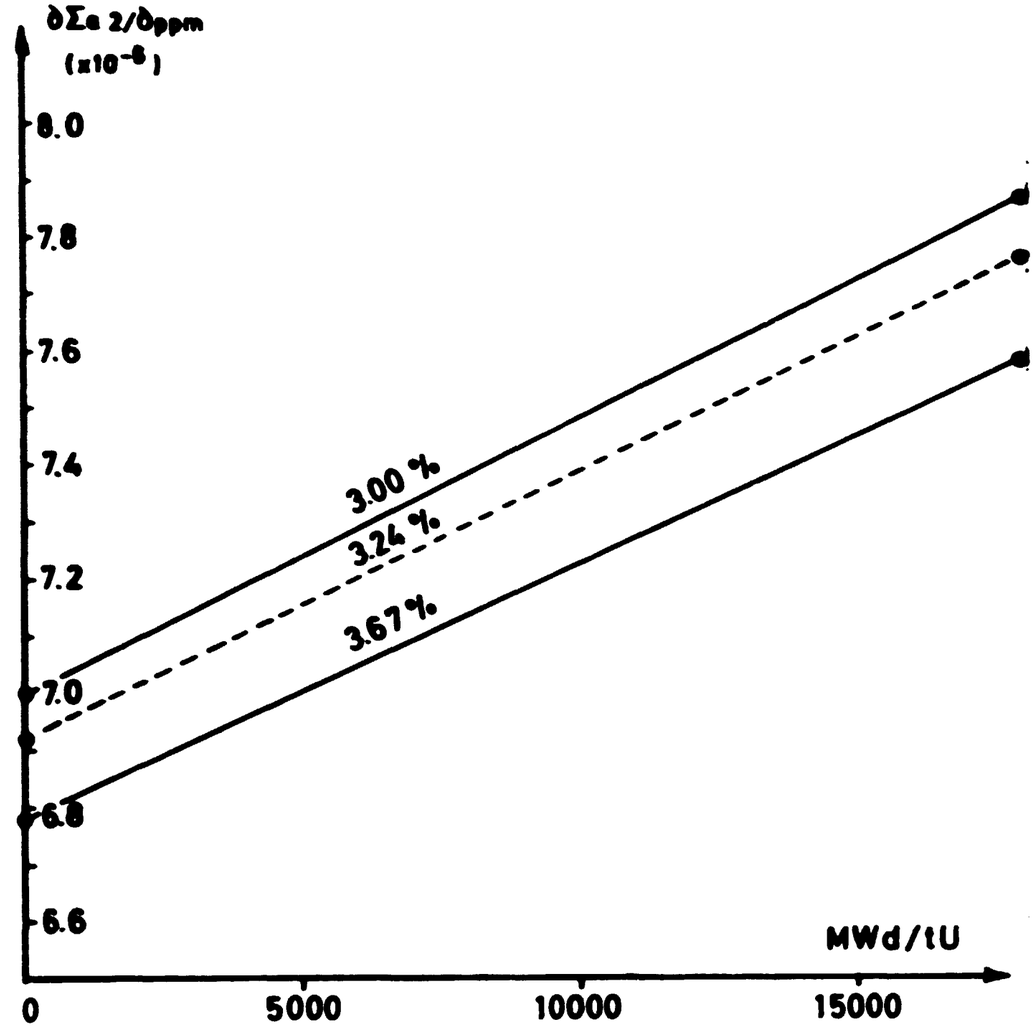

Fig. 7.5.c. HFP 1000 ppm values of coolant boron worth versus burn-up and initial fuel enrichments.

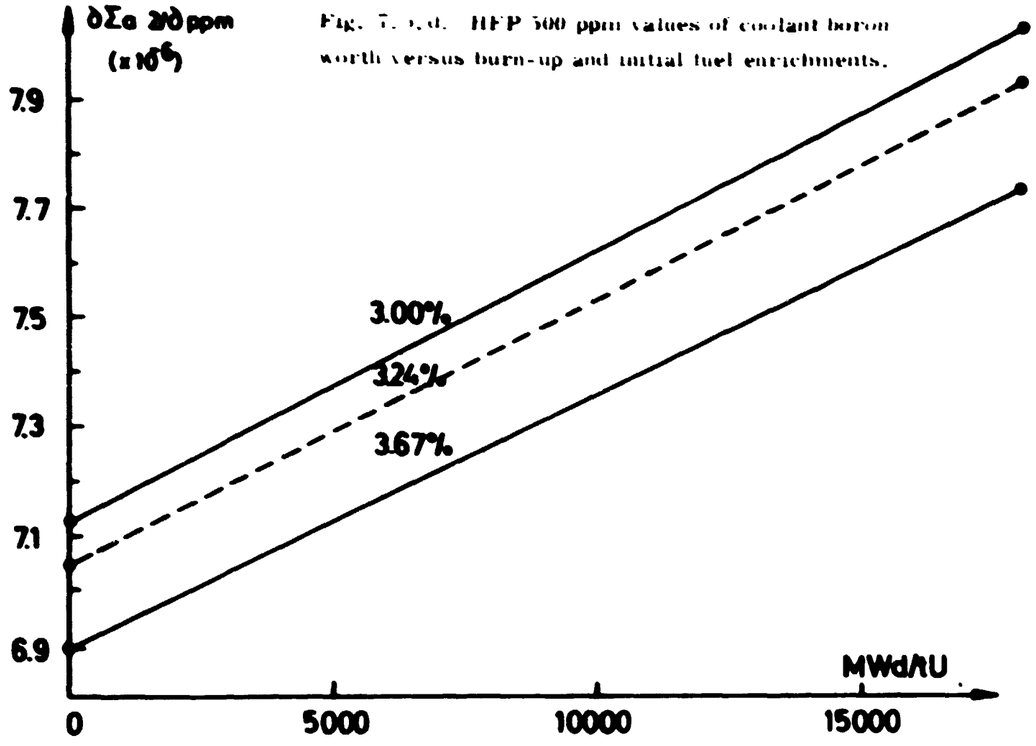

Fig. 7.5.d. HFP 500 ppm values of coolant boron worth versus burn-up and initial fuel enrichments.

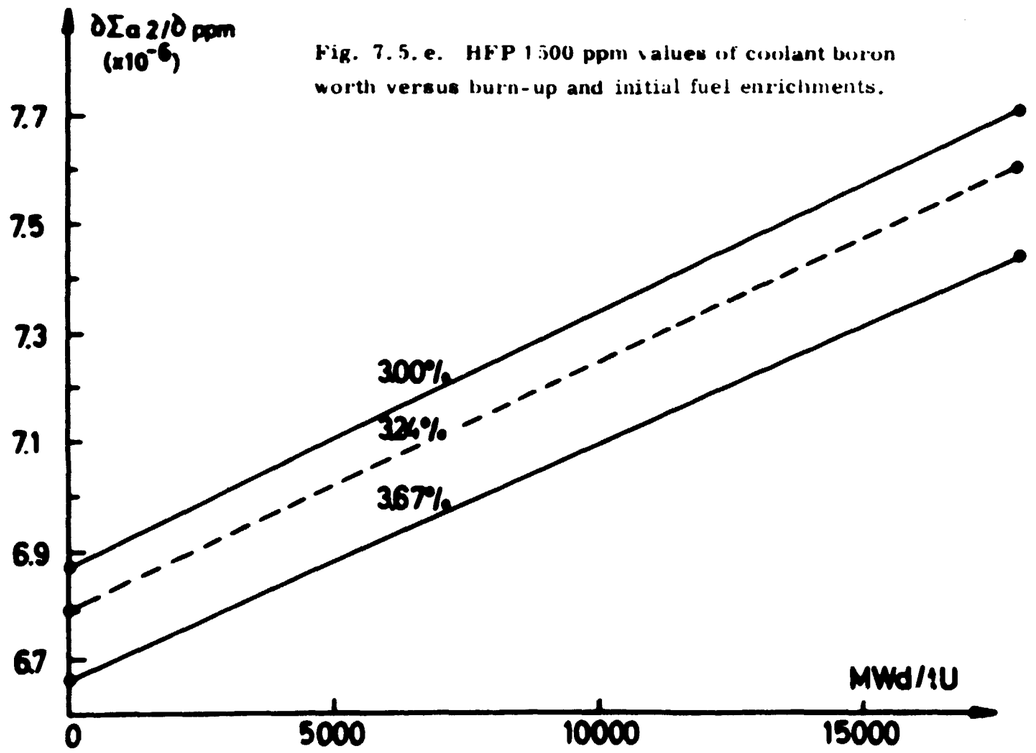

Fig. 7.5.e. HFP 1500 ppm values of coolant boron worth versus burn-up and initial fuel enrichments.

8. BURN-UP CALCULATIONS ON THE FIRST CY CORE LOADING

8.1. Investigations of Poison Coefficients to be Used in DBU Burn-up Calculations

Ref. 5 describes measurements of the relative power sharing of each fuel assembly. Figs. 8.1.a-b show the results of measurements at 2030 and 9850 MWd/tU. Furthermore the figures show mean values of measurements in symmetrical positions, which were compared with Risø CRS/GP/CDB/DBU calculations at a power level of 1465 MWT with poison coefficients as defined in a, b, and c in 7.5. For small burn-up values (2030 MWd/tU), the agreement between measurements and calculations is within a few per cent in all three cases. Case b is shown in fig. 8.1.c. For higher burn-up values (9850 MWd/tU), the agreement between measurements and calculations is satisfactory in case a (constant values of $\partial\Sigma_a^B/\partial$ ppm), but much better in cases b (fig. 8.1.d) and c, where the agreement is very good.

No measurements at high burn-up values (18,000-20,000 MWd/tU) were available, but comparison between Risø calculations in fig. 8.1.e shows a marked discrepancy (up to 20%) between power distributions calculated with constant $\partial\Sigma_{a2}^B/\partial$ppm values (case a) and $\partial\Sigma_{a2}^B/\partial$ppm values as functions of initial enrichment and burn-up (case b). Calculations at high burn-up values showed, however, only a minor difference between power distributions calculated with $\partial\Sigma_{a2}^B/\partial$ ppm = f (initial enrichment, burn-up) and $\partial\Sigma_{a2}^B/\partial$ppm = f (initial enrichment, burn-up, ppm concentration level) - (cases b and c).

From the calculations mentioned above the following conclusions are drawn: A constant value of $\partial\Sigma_{a2}^B/\partial$ppm, independent of initial enrichment and burn-up, gives misleading results at higher and high burn-up values. Coefficients as functions of initial enrichment and burn-up (case b) appear to give good agreement between measurements and calculations. It is not necessary to use coefficients where the coolant ppm concentration level is used as a parameter. Coefficients evaluated at a mean ppm concentration level (~1000 ppm) are sufficient.

Figs. 8.1.f-g show examples of comparisons between Risø calculations with poison coefficients as functions of initial enrichment and burn-up (case b) and Westinghouse calculations[2]. On comparison of these results with figs. 8.1.c-d it is seen that the agreement between Westinghouse measurements, Westinghouse calculations, and Risø calculations is good, in most positions within a few per cent.

Fig. 8.1.h shows the radial assembly form factors versus burn-up. Again the agreement is good, although at higher burn-up values there is a tendency for the calculated power distributions to be a little more flat (lower form factors) than the measurements show.

More detailed information on the calculations mentioned above is given in ref. 30.

It should be mentioned that the calculations described in this section are based on CDB cross sections as functions of burn-up, calculated at the mean box power level (~ 0.03 MW/cm box). A series of calculations showed[30] that the influence of the power level - at which the CDB cross sections to be used in DBU are calculated - on the power distributions was of minor importance. The difference in power distributions calculated with mean power cross sections and power level dependent cross sections is even at high burn-up values of the order of 2%.

8.2. Critical Boron Concentrations during Burn-up

Fig. 8.2.a shows the Westinghouse measured and predicted "All Rods Out" critical boron concentration as a function of core burn-up together with Risø DBU calculated values. The agreement between Westinghouse and Risø values is good at higher burn-up values. At small burn-up values the Risø calculations seem to overestimate the critical boron concentration by about 1 % ∂k/k.

8.3. Plutonium Production during Burn-up

Fig. 8.3.a shows the region burn-up versus average core burn-up, calculated with DBU. This figure together with fig. 8.3.b, which shows CDB calculations of the total Pu production in each region versus burn-up, was used to calculate the specific Pu production in each region as a function of the average core burn-up (fig. 8.3.d). Similarly figs. 8.3.a and 8.3.c were used in fig. 8.3.e, where the ratio fissile Pu/total Pu versus the average burn-up is given.

For comparison the Westinghouse calculations from ref. 2 are shown also in figs. 8.3.d-e.

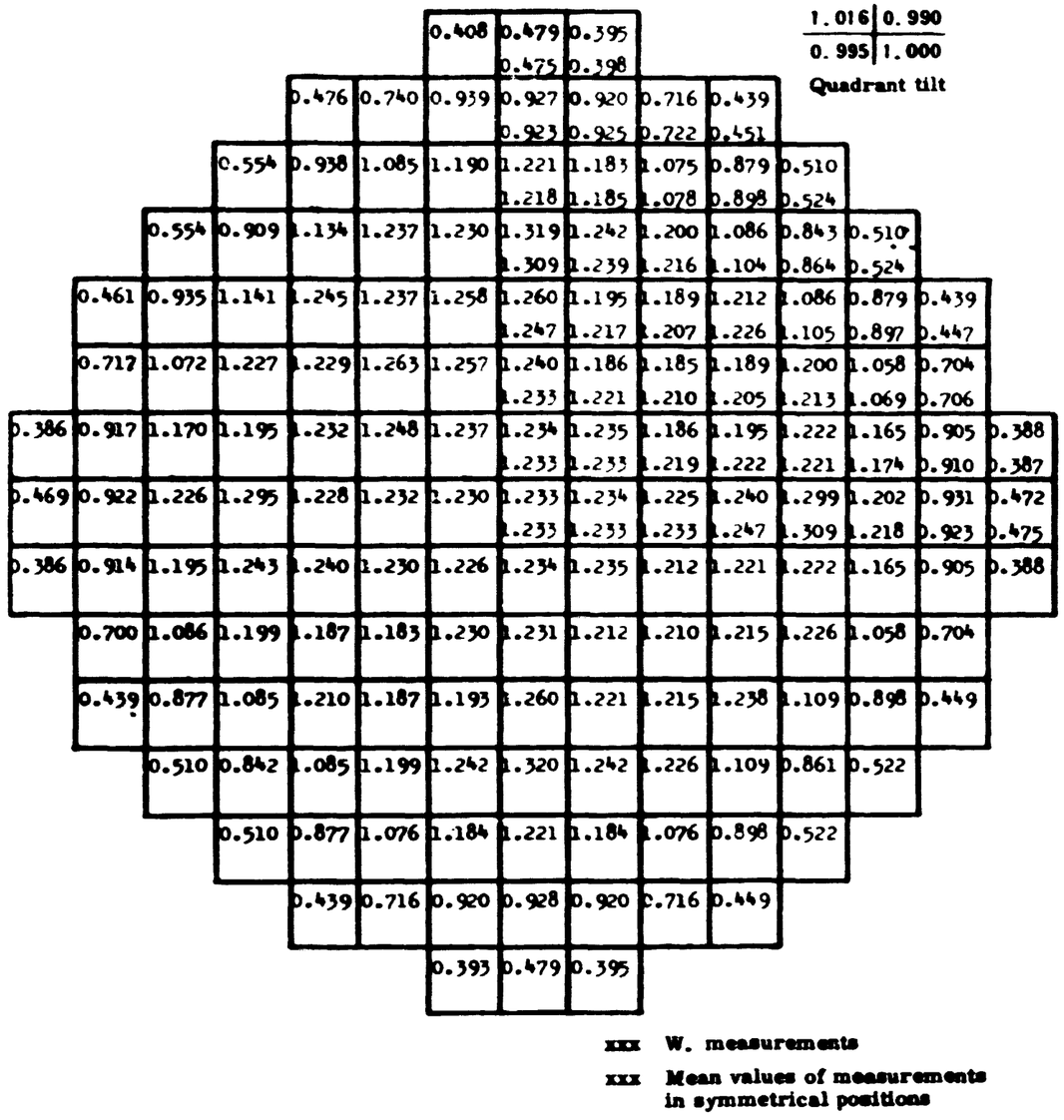

Fig. 8.1.a. CY relative power distribution. 2030 MWd/tU.

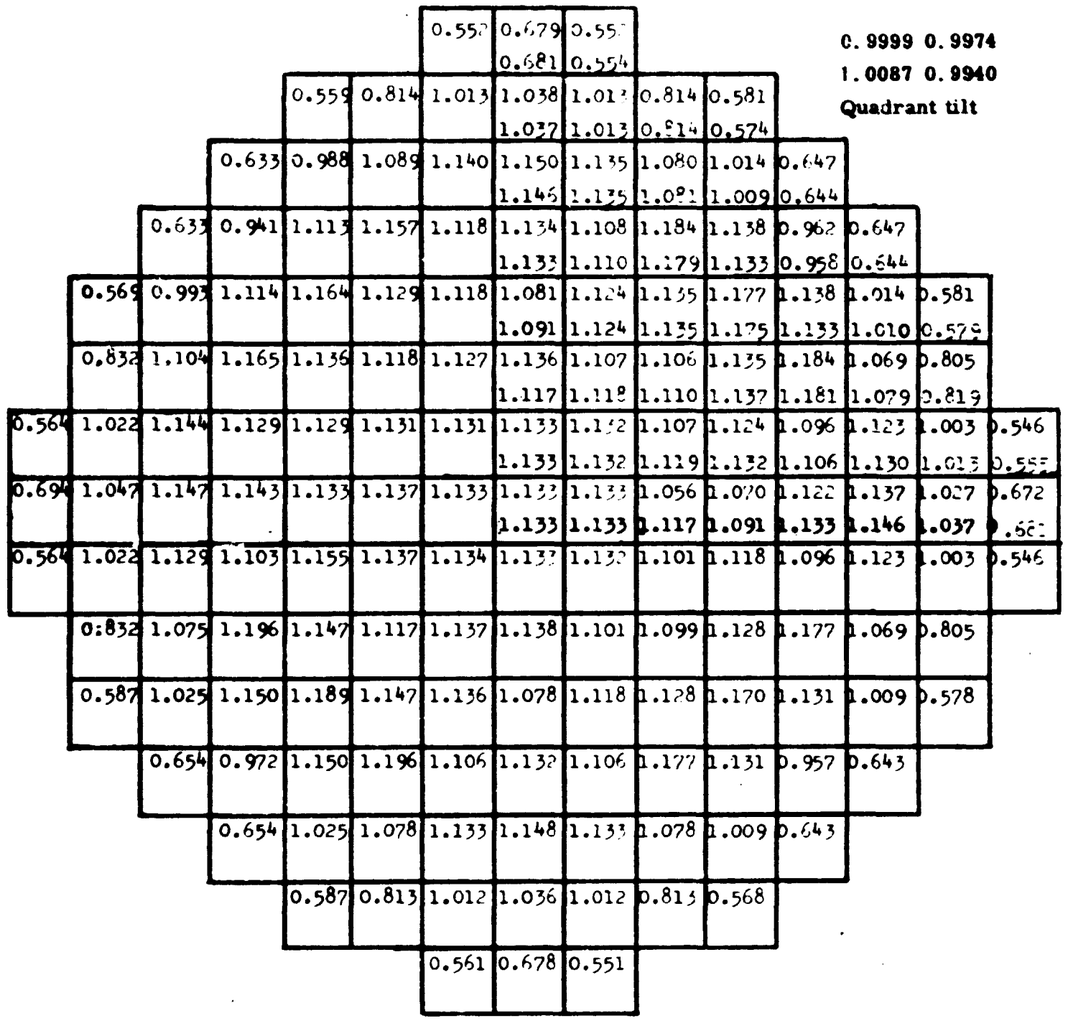

Fig. 8.1.b. CY relative power distribution. 9850 MWd/tU.

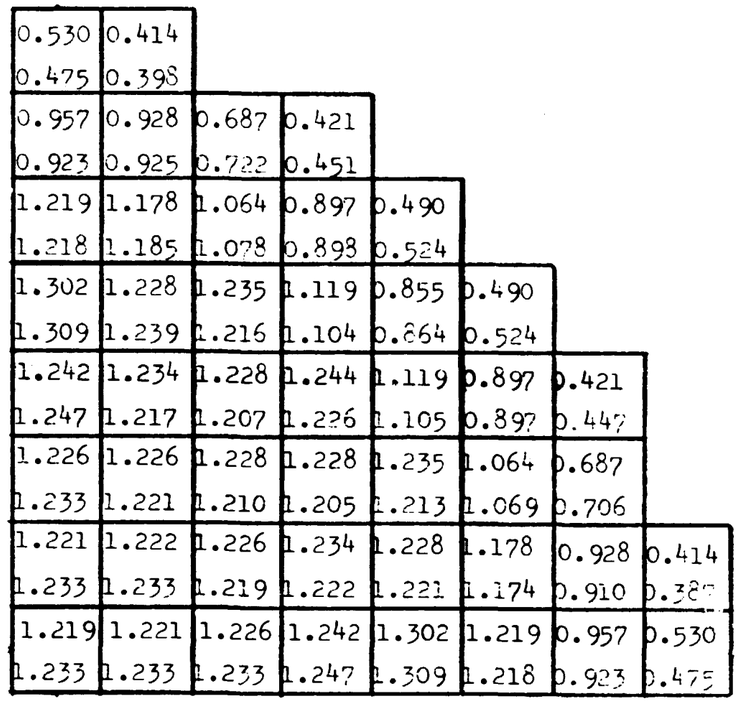

xxx Risø 2D calculations

xxx W. measurements (mean values)

Fig. 8.1.c. CY relative power distribution. 2030 MWd/tU.
$\partial \Sigma^{B}_{a2}/\partial$ ppm = f (initial enrichment, burn-up).

0.686	0.547						
0.681	0.554						
1.053	1.026	0.805	0.539				
1.037	1.013	0.814	0.574				
1.185	1.164	1.100	0.988	0.608			
1.146	1.135	1.081	1.009	0.644			
1.190	1.147	1.176	1.127	0.946	0.608		
1.133	1.110	1.179	1.133	0.958	0.644		
1.125	1.125	1.135	1.175	1.127	0.988	0.539	
1.091	1.124	1.135	1.175	1.133	1.010	0.579	
1.106	1.109	1.118	1.135	1.176	1.100	0.805	
1.117	1.118	1.110	1.137	1.181	1.079	0.819	
1.100	1.102	1.109	1.125	1.147	1.164	1.026	0.547
1.133	1.132	1.119	1.132	1.106	1.130	1.013	0.555
1.098	1.100	1.106	1.125	1.190	1.185	1.053	0.686
1.133	1.133	1.117	1.091	1.133	1.146	1.037	0.681

xxx Risø 2D calculations

xxx W. measurements (mean values)

Fig. 8.1.d. CY relative power distribution. 9850 MWd/tU. $\partial\Sigma^{B}_{a2}/\partial$ppm = f (initial enrichment, burn-up).

0.822	0.741						
0.762	0.654						
1.089	1.094	1.006	0.812				
1.058	1.043	0.899	0.679				
1.104	1.108	1.110	1.087	0.842			
1.121	1.115	1.089	1.029	0.740			
1.053	1.035	1.087	1.104	1.033	0.842		
1.109	1.084	1.118	1.103	0.992	0.740		
0.984	0.991	1.015	1.077	1.104	1.087	0.812	
1.066	1.068	1.078	1.116	1.103	1.029	0.679	
0.961	0.966	0.983	1.015	1.087	1.110	1.006	
1.059	1.061	1.066	1.078	1.118	1.089	0.899	
0.952	0.955	0.966	0.991	1.035	1.108	1.094	0.741
1.058	1.059	1.061	1.068	1.084	1.115	1.043	0.654
0.950	0.952	0.961	0.984	1.053	1.104	1.089	0.822
1.058	1.058	1.059	1.066	1.109	1.121	1.058	0.762

xxx Constant value of $\partial\Sigma^{B}_{a2}/\partial$ppm

xxx $\partial\Sigma^{B}_{a2}/\partial$ppm = f (initial enrichment, burn-up)

Fig. 8.1.e. CY relative power distribution. 19730 MWd/tU. DBU calculations.

0.521 0.53	0.405 0.43						
0.960 0.95	0.934 0.94	0.683 0.73	0.412 0.47				
1.241 1.22	1.195 1.18	1.071 1.07	0.897 0.92	0.479 0.54			
1.324 1.30	1.240 1.21	1.250 1.24	1.126 1.12	0.847 0.87	0.479 0.54		
1.241 1.22	1.233 1.21	1.231 1.21	1.257 1.24	1.126 1.12	0.897 0.92	0.412 0.47	
1.210 1.19	1.212 1.19	1.220 1.20	1.231 1.21	1.250 1.24	1.071 1.07	0.683 0.73	
1.197 1.17	1.200 1.18	1.212 1.19	1.233 1.21	1.240 1.21	1.195 1.18	0.934 0.94	0.405 0.43
1.193 1.17	1.197 1.17	1.210 1.19	1.241 1.22	1.324 1.30	1.241 1.22	0.960 0.94	0.521 0.53

xxx Risø 2D calculations

xxx Westinghouse 2D calculations

Fig. 8.1.f. CY relative power distribution. No burn-up.

0.707 0.73	0.570 0.61						
1.056 1.06	1.03 1.05	0.821 0.87	0.562 0.62				
1.170 1.15	1.153 1.14	1.097 1.09	0.996 1.02	0.631 0.69			
1.171 1.14	1.133 1.11	1.163 1.14	1.122 1.11	0.956 0.98	0.631 0.69		
1.113 1.08	1.114 1.09	1.124 1.10	1.163 1.14	1.122 1.11	0.996 1.02	0.562 0.62	
1.100 1.07	1.102 1.07	1.109 1.08	1.124 1.10	1.163 1.14	1.097 1.09	0.821 0.87	
1.096 1.07	1.097 1.07	1.102 1.07	1.114 1.09	1.133 1.11	1.153 1.14	1.03 1.05	0.570 0.61
1.096 1.06	1.096 1.07	1.100 1.07	1.113 1.08	1.171 1.14	1.170 1.15	1.056 1.06	0.707 0.73

xxx Risø 2D calculations

xxx Westinghouse 2D calculations

Fig. 8.1.g. CY relative power distribution. 12100 MWd/tU.

Fig. 8.1.b. "All Rods Out" radial assembly power form factors versus burn-up (1465 MWT).

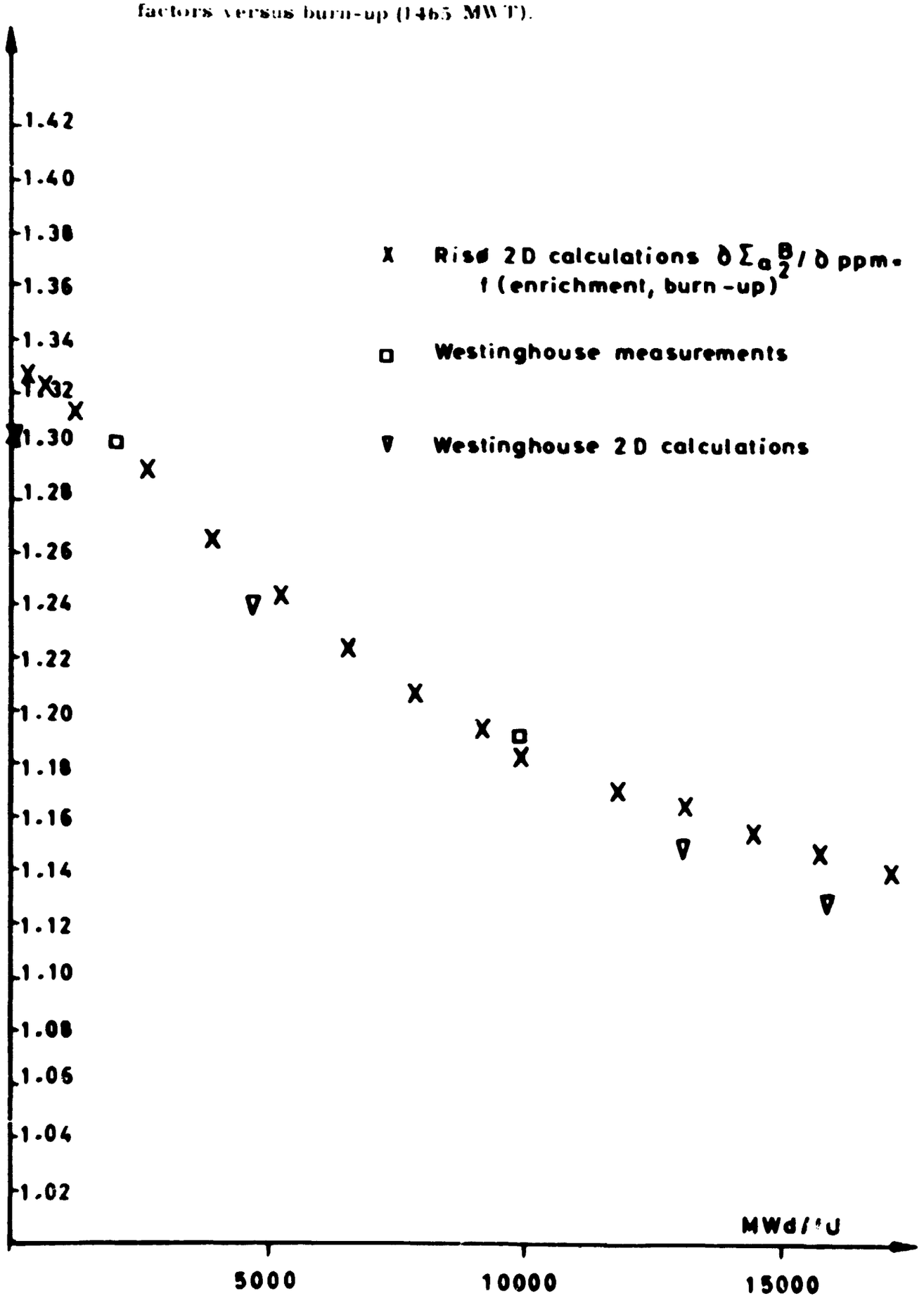

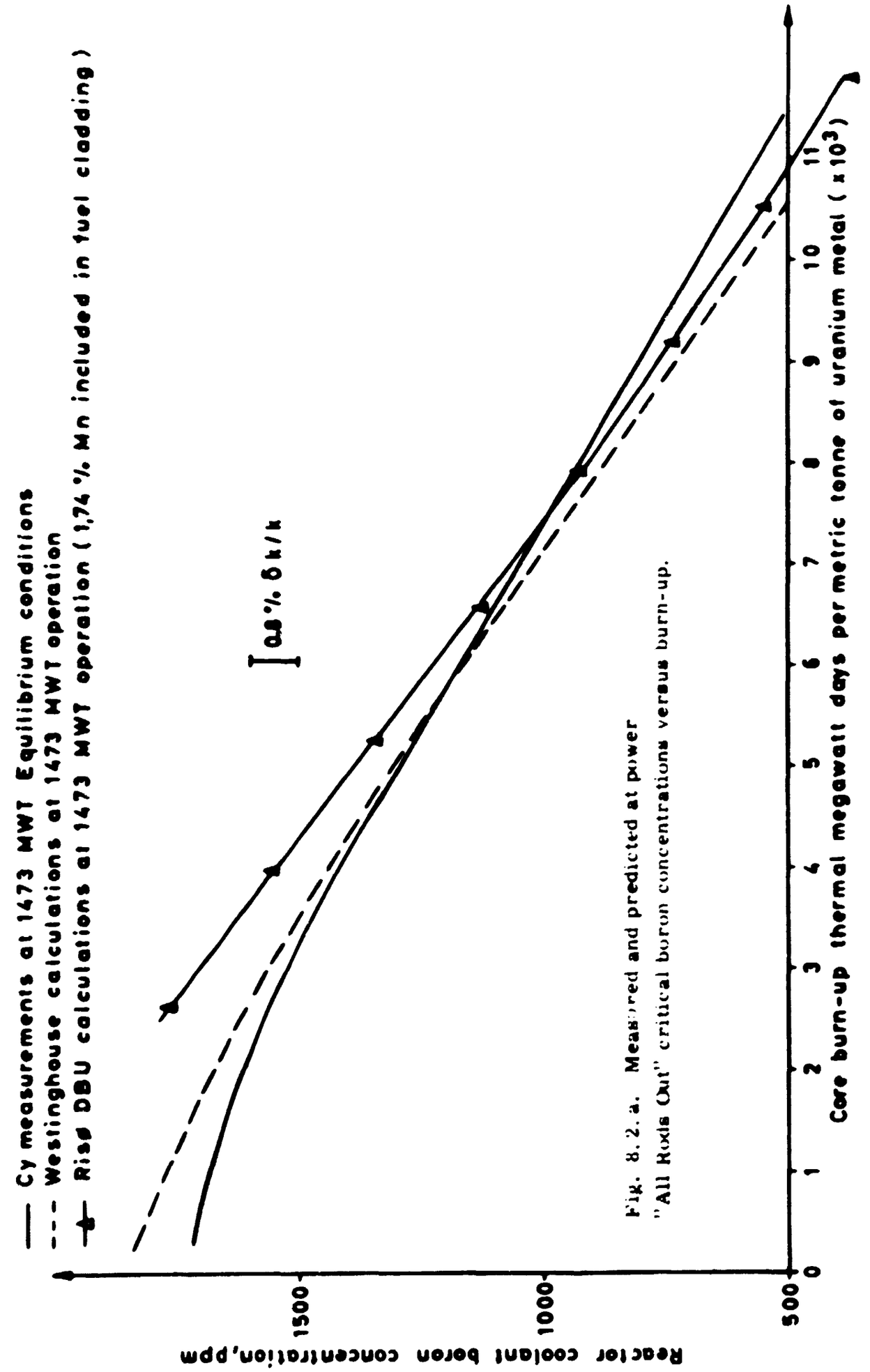

Fig. 8.2.a. Measured and predicted at power "All Rods Out" critical boron concentrations versus burn-up.

Fig. 8.3.a. Region burn-up versus average core burn-up.

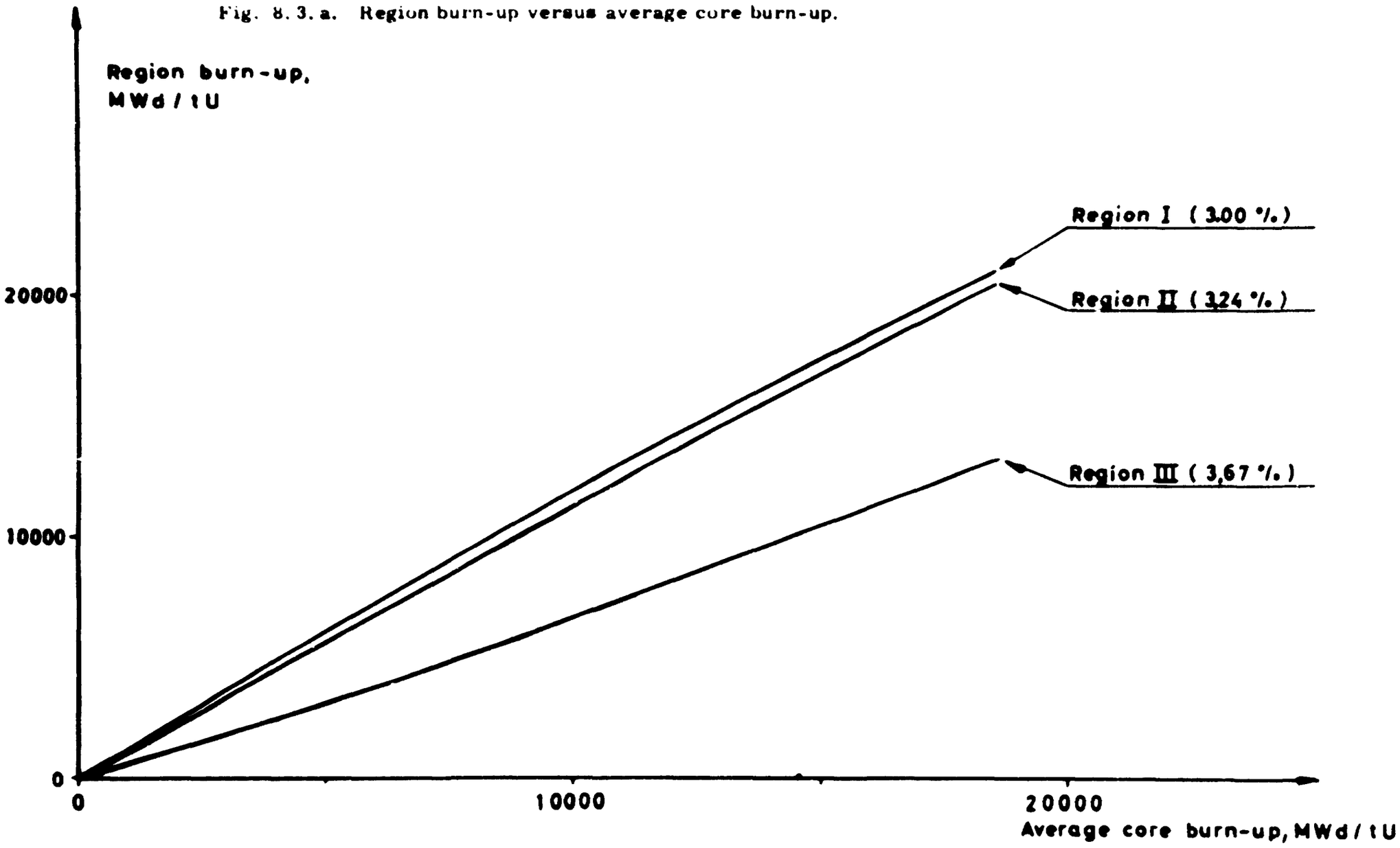

Fig. 8.3.b. Specific Pu production versus burn-up for each region.

Fig. 8.3.c. Fissile Pu/total Pu versus burn-up. Risø CDB calculations.

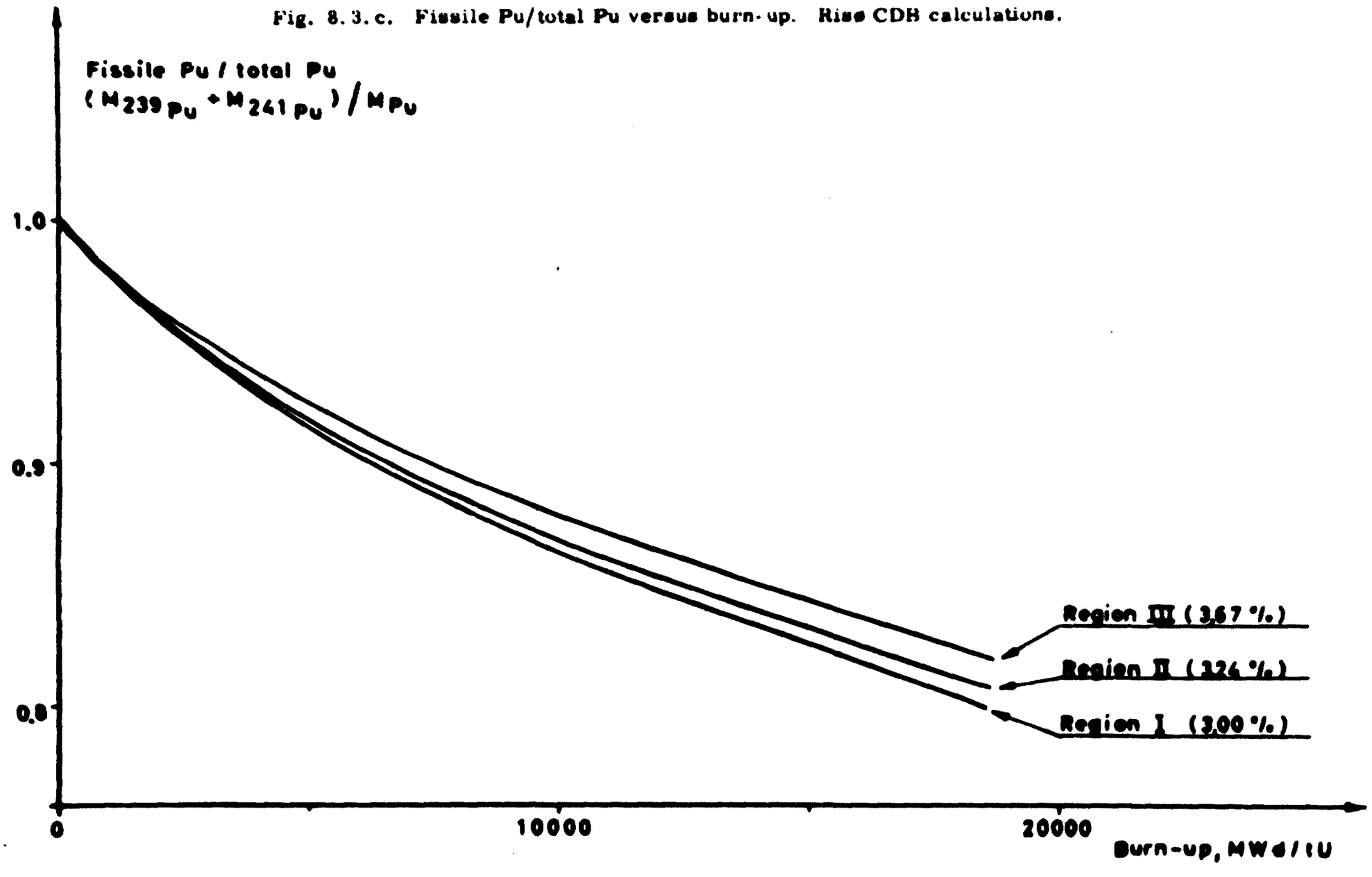

Fig. 8.3.d. Specific Pu production versus core burn-up for each region.

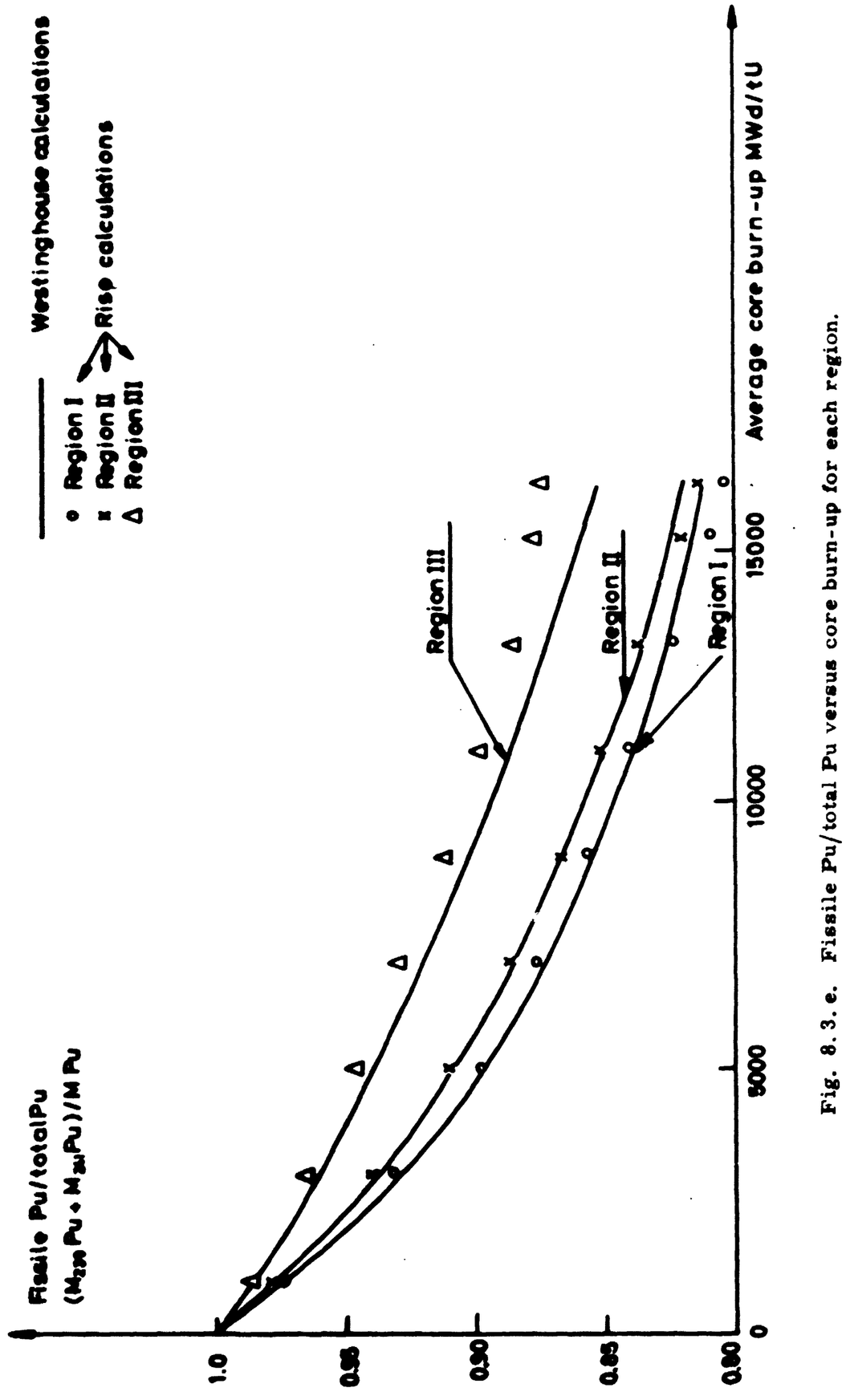

Fig. 8.3.e. Fissile Pu/total Pu versus core burn-up for each region.

9. CONCLUSION

As mentioned in the introduction the calculations reported here were performed in order to check the reliability of the calculation system including the cross section data.

The results obtained are generally speaking quite satisfactory and have so to speak "come naturally" since no special effort, as mentioned in 2.7, has been made in fitting the cross sections for light-water reactor calculations.

In conjunction with the results reported in refs. 7, 8, and 11 these results may inspire a reasonable degree of confidence in the entire calculation system as regards calculations on light-water power reactors.

However, certain aspects qualify for further research and development. As an example may be mentioned the shortcommings described in ref. 11, when larger concentrations of plutonium is present, which will be the case by Pu-recycling. An inkling of these shortcomings is given by the overestimation of the plutonium production which appears in figs. 8.3.d-e.

ACKNOWLEDGEMENTS

The authors wish to thank the members of the Reactor Physics Department, Risø for assistance and valuable discussions. Especially we want to thank Mrs. Liselotte K. Meltofte, who with great care assisted in the EDP work.

REFERENCES

1) Connecticut Yankee Atomic Power Company: Facility Description and Safety Analysis. NYO-3250-5, DOCKET 50213-5. (1966) Vol. 1-2.

2) J.D. McGaugh, The Nuclear Design of the Connecticut-Yankee Reactor. NYO-3250-27 (1968) 129 pp.

3) I.H. Coen, Reference Core Design for the Connecticut Yankee Atomic Power Company Haddam Connecticut Reactor. NYO-3250-39 (1967) 77 pp.

4) James R. Himmelwright, The Startup Test Program for the Connecticut Yankee Reactor. NYO-3250-11 (1967) 37 pp.

5) James R. Himmelwright, Reactor and Plant Performance Engineering Tests and Measurements. DOCKET-50213-25 (1969) 126 pp.

6) Z.R. Rosztoczy and R. Kern, Setup of Isocheck Method for Determining Heavy-Isotope Content in the Operating Fuel Elements of Connecticut Yankee Core I. CEND-287 (1966) 38 pp.

7) A.M. Hvidtfeldt Larsen, H. Larsen, and T. Petersen, Calculations on a Boiling Water Reactor as a Test of the Risø Reactor Code Complex. Risø Report No. 268 (1972) 102 pp.

8) Hans Larsen, Three-dimensional Boiling-Water Reactor Neutron Flux Calculations on the Basis of Homogenized Fuel Box Cross Sections. Risø-M-1616 (1973) 17 pp.

9) K.E. Lindstrøm Jensen, Development and Verification of Nuclear Calculation Methods for Light Water Reactors. Risø Report No. 235 (1971) 165 pp.

10) B. Micheelsen, Review of the Situation in Burn-Up Physics - as seen from Denmark. Reactor Burn-Up Physics, Proceedings of a Panel, Vienna, 12-16 July 1971 (IAEA, Vienna, 1973) 23-37.

11) A.M. Hvidtfeldt Larsen, Multigroup Cross Sections for Reactor Physics Calculations, Generated on the Basis of Fundamental Nuclear Data. Risø Report No. 286 (1973) 63 pp.

12) D.S. Norton, The UKAEA Nuclear Data Library, Februar 1968. AEEW-M824 (1968) 23 pp.

13) K. Parker, The Aldermaston Nuclear Data Library as at May 1963. AWRE 0-70/63 (1963) 64 pp.

14) Jørn Mikkelsen, The Neutron Resonance Reactions in Thermal Nuclear Reactors Determined by Semi-Analytic as well as Numerical Methods. Risø Report No. 234 (1970) 167 pp.

15) J. Petersen, A Preliminary Description of the SIGMA Programme. Risø-M-949 (1969). Internal report.

16) A.M. Hvidtfeldt Larsen, SIGMA MASTER TAPE, a Multigroup Cross Section Library. Risø Report No. 262 (1972) 50 pp.

17) R.J. Brissenden and C. Durston, A User's Guide to GENEX, SDR, and Related Computer Codes. AEEW-R 622 (1968) 177 pp.

18) J.R. Askew, The Calculation of Resonance Captures in a Few Group Approximation. AEEW-R-489 (1966) 22 pp.

19) H. Neltrup, RESOREX, A Procedure for Calculating Resonance Group Cross-Sections. Risø-M-1437 (1971) 25 pp.

20) H. Larsen, Approximate Methods for 3D Overall Calculations on Light Water Reactors. Risø Report 270 (1972) 48 pp.

21) J. Pedersen, Calculation of Heterogeneous Constants for Cylinders and Slabs. Risø-M-850 (1969) 20 pp.

22) F.J. Fayers, P.B. Kemshell, and M.J. Terry, An Evaluation of some Uncertainties in the Comparison between Theory and Experiment for Regular Light Water Lattices. J. Brit. Nucl. Energy. Soc 6 (1967) 161-181.

23) Per B. Suhr, Connecticut Yankee (Haddam Neck) Reactor Core Characteristics. CY-1, Internal Report R.Ph. 199 (1972).

24) T. Lyman (editor), Metals Handbook. Vol. I, 8th edition (American Society for Metals, Metals Park, Novelty, Ohio, 1961).

25) Ernst Schmidt, Properties of Water and Steam in SI-Units (Springer, Berlin, 1969) 205 pp.

26) T. Leffers, Metallurgy Dep., Risø. Private Communication, 1972.

27) Per B. Suhr, Survey of Calculations on the Haddam Neck (Connecticut Yankee). Power Plant with the Risø Reactor Code System. Risø-M-1619 (1973). Internal report.

28) H. W. Graves, R. F. Janz, and C. G. Poncelet, The Nuclear Design of the Yankee Core (Yankee Rowe). YAEC-136 (1961) 91 pp.

29) Per B. Suhr, Haddam Neck (Connecticut Yankee) Power Plant. Calculations of Reactivity and Poison Coefficients, CY-3, Internal report R. Ph. 200 (1973).

30) Per B. Suhr, Haddam Neck (Connecticut Yankee) Power Plant. Burn-up Calculations, CY-5, Internal Report R. Ph. 205 (1973).

APPENDIX

DANCOFF FACTOR FOR A CELL CONTAINING HEAVY SCATTERING ATOMS

Consider the case of three regions (fig. 6.1.b), in which one outer region with volume V_f contains only heavy nuclides giving a macroscopic scattering cross section, Σ_f^c, and one moderator region with volume V_m containing both light nuclides with macroscopic scattering cross sections, Σ_m^s, as well as heavy nuclides contributing Σ_m^c to the total macroscopic scattering cross section $\Sigma_m = \Sigma_m^c + \Sigma_m^s$.

The third region, the control rod region, with volume V_c, the Dancoff factor of which is going to be calculated, only appears indirectly in the calculation as it is assumed black, in actual fact provided with a very high macroscopic absorption cross section, 10^5 cm^{-1}.

On these premises the slowing down equations for the fluxes ϕ_m and ϕ_f in the volumes V_m and V_f may in the usual notation be written:

$$\phi_m V_m \Sigma_m = P_{mf} V_f \int_E^{E/a_f} \phi_f \Sigma_f^c \frac{dE'}{(1-a_f^c)E'} + P_{mm} V_m \int_E^{E/a_m^c} \phi_m \Sigma_m^c \frac{dE'}{(1-a_m^c)E'}$$

$$+ P_{mm} V_m \int_E^{E/a_m^s} \phi_m \Sigma_m^s \frac{dE'}{(1-a_m^s)E'} ,$$

$$\phi_f V_f \Sigma_f^c = P_{ff} V_f \int_E^{E/a_f} \phi_f \Sigma_f^c \frac{dE'}{(1-a_f^c)E'} + P_{fm} V_m \int_E^{E/a_m^c} \phi_m \Sigma_m^c \frac{dE'}{(1-a_m^c)E'}$$

$$+ P_{fm} V_m \int_E^{E/a_m^s} \phi_m \Sigma_m^s \frac{dE'}{(1-a_m^s)E'}$$

P_{ij} is the probability that a neutron born in region j makes its first collision in region i.

When the first and second integral in both equations are treated in the WR-approximation and the last integral in the NR-approximation, and the reciprocity relation $V_m \cdot \Sigma_m P_{fm} = V_f \Sigma_f^c P_{mf}$ is used, the following expressions are found:

$$\phi_m = P_{fm}\phi_f + P_{mf}\frac{\Sigma_m^c}{\Sigma_m}\phi_m + P_{mm}\frac{\Sigma_m^s}{\Sigma_m}\cdot\frac{1}{E}$$

$$\phi_f = P_{ff}\phi_f + P_{mf}\frac{\Sigma_m^c}{\Sigma_m}\phi_m + P_{mf}\frac{\Sigma_m^s}{\Sigma_m}\cdot\frac{1}{E}$$

From these two linear equations ϕ_m and ϕ_f can be found and the Dancoff factor, d_c, for region V_c may then be calculated as:

$$d_c = \left(\left(\frac{\Sigma_m^s}{E} + \phi_m \Sigma_m^c\right)\right) V_m P_{cm} + \phi_f \Sigma_f^c V_f P_{cf}) \Big/ \left(\frac{S_c}{4}\cdot\frac{1}{E}\right)$$

The numerator gives the number of neutrons that hit the surface S_c of V_c and the denominator the number that would hit the surface S_c if immersed in an infinite medium with a flat 1/E-flux. The expression for d_c when ϕ_m and ϕ_c are inserted will not contain E.

ISBN 87 550 0228 5